JOURNAL OF GEOPHYSICAL RESEARCH, VOL. 113, D16S43, doi:10.1029/2007JD008824, 2008

High Resolution Dynamics Limb Sounder: Experiment overview, recovery, and validation of initial temperature data

John Gille,[1,2] John Barnett,[3] Philip Arter,[1,4] Marion Barker,[5] Peter Bernath,[6,7] Chris Boone,[6] Charles Cavanaugh,[2] Jonathan Chow,[5] Michael Coffey,[2] James Craft,[1] Cheryl Craig,[2] Michael Dials,[1,8] Vincil Dean,[1] Thomas Eden,[2] D. P. Edwards,[2] Gene Francis,[2] Chris Halvorson,[2] Lynn Harvey,[9] Christopher Hepplewhite,[3] Rashid Khosravi,[2] Douglas Kinnison,[2] Charles Krinsky,[1] Alyn Lambert,[2,10] Hyunah Lee,[2,11] Lawrence Lyjak,[2,12] Joanne Loh,[1] William Mankin,[2,13] Steven Massie,[2] Joseph McInerney,[1,2] Joseph Moorhouse,[3] Bruno Nardi,[2] Daniel Packman,[2] Cora Randall,[9] Jolyon Reburn,[14] Wayne Rudolf,[5] Michael Schwartz,[10] John Serafin,[5] Kenneth Stone,[1,15] Brendan Torpy,[1] Kaley Walker,[6,16] Alison Waterfall,[14] Robert Watkins,[3] John Whitney,[3,13] Douglas Woodard,[1,17] and Gregory Young[1]

Received 15 April 2007; revised 27 January 2008; accepted 1 April 2008; published 27 June 2008.

[1] The High Resolution Dynamics Limb Sounder (HIRDLS) experiment was designed to provide global temperature and composition data on the region from the upper troposphere to the mesopause with vertical and horizontal resolution not previously available. The science objectives are the study of small-scale dynamics and transports, including stratosphere-troposphere exchange, upper troposphere/lower stratosphere chemistry, aerosol, cirrus and PSC distributions, and gravity waves. The instrument features 21 channels, low noise levels, high vertical resolution, and a mechanical cooler for long life. During launch most of the optical aperture became obscured, so that only a potion of an optical beam width at a large azimuth from the orbital plane on the side away from the Sun can see the atmosphere. Irrecoverable loss of capabilities include limitation of coverage to the region 65°S–82°N and inability to obtain longitudinal resolution finer than an orbital spacing. While this optical blockage also impacted radiometric performance, extensive effort has gone into developing corrections for the several effects of the obstruction, so that radiances from some of the channels can be put into retrievals for temperature. Changes were also necessary for the retrieval algorithm. The validation of the resulting temperature retrievals is presented to demonstrate the effectiveness of these corrections. The random errors range from ~0.5 K at 20 km to ~1.0 at 60 km, close to those predicted. Comparisons with high-resolution radiosondes, lidars, ACE-FTS, and ECMWF analyses give a consistent picture of HIRDLS temperatures being 1–2 K warm from 200 to 10 hPa and within ±2 K of standards from 200 to 2 hPa (but warmer in the region of the tropical tropopause), above which HIRDLS appears to be cold. Comparisons show that both COSMIC and HIRDLS can see small vertical features down to about 2 km

[1]Center for Limb Atmospheric Sounding, University of Colorado, Boulder, Colorado, USA.
[2]National Center for Atmospheric Research, Boulder, Colorado, USA.
[3]Department of Physics, Oxford University, Oxford, UK.
[4]Deceased 20 April 2003.
[5]Lockheed Martin Advanced Technology Center, Palo Alto, California, USA.
[6]Department of Chemistry, University of Waterloo, Waterloo, Ontario, Canada.
[7]Now at Department of Chemistry, University of York, York, UK.
[8]Now at Ball Aerospace and Technologies Corporation, Boulder, Colorado, USA.
[9]Laboratory for Atmospheric and Space Physics, University of Colorado, Boulder, Colorado, USA.
[10]Jet Propulsion Laboratory, California Institute of Technology, Pasadena, California, USA.
[11]Deceased 6 July 2007.
[12]Now at National Weather Service, NOAA, Silver Spring, Maryland, USA.
[13]Retired.
[14]Rutherford Appleton Laboratory, Didcot, UK.
[15]Now at ERT, Inc., Aurora, Colorado, USA.
[16]Now at Department of Physics, University of Toronto, Toronto, Ontario, Canada.
[17]Deceased 2 February 2005.

0148-0227/08/2007JD008824$09.00

wavelength. While further improvements in the data are expected, these data will allow HIRDLS to provide important support toward reaching the Aura objectives.

Citation: Gille, J., et al. (2008), High Resolution Dynamics Limb Sounder: Experiment overview, recovery, and validation of initial temperature data, *J. Geophys. Res.*, *113*, D16S43, doi:10.1029/2007JD008824.

1. Introduction

[2] Space-based experiments have contributed much to our knowledge of the stratosphere in recent years. These observations have been characterized by large horizontal or vertical scales, leaving a range of unobserved phenomena at smaller scales. This is especially true at the tropopause, the boundary between the troposphere and stratosphere, where rapid vertical changes in temperature and composition have been unobserved on a global basis.

[3] The High Resolution Dynamics Limb Sounder (HIRDLS) experiment was designed to address problems for which these scales are important. HIRDLS is a 21 channel limb-scanning infrared radiometer designed to make global measurements at smaller vertical and horizontal scales than have been previously observed, from pole to pole, at altitudes of 8–80 km.

[4] It is the result of the collaborative efforts of scientists and engineers in three groups: the Atmospheric, Oceanic and Planetary Physics group from Oxford University in the United Kingdom, the Center for Limb Atmospheric Sounding of the University of Colorado at Boulder, and the Atmospheric Chemistry Division of the National Center for Atmospheric Research, also in Boulder. Work on HIRDLS began with separate proposals to NASA in 1988. While some of the instrumental details were different, their scientific objectives were similar, and the groups agreed to work together on a single experiment. The experiment was selected for flight as part of the Earth Observing System (EOS) program, and later assigned to the Aura spacecraft. Section 2 of this paper outlines the scientific objectives of the experiment, and section 3 gives a brief description of the most salient features of the instrument.

[5] During launch an unfortunate accident occurred, resulting in a blockage of most of the optical aperture, significantly reducing the coverage and longitudinal resolution. These are described in section 4. Section 5 notes the effects of the blockage on the radiometric performance, and provides a brief outline of the algorithms that have been developed to correct for the blockage and recover some of the radiances, followed by an outline of the retrieval algorithm in section 6. A measure of the success of this data recovery effort is demonstrated by the validation of the present Version 2.04.09 temperature results, presented in section 7. Section 8 describes the determination of the vertical resolution of the HIRDLS data through comparisons with COSMIC data, while section 9 summarizes the accuracy and precision of HIRDLS temperature at this stage. The capabilities of the HIRDLS experiment and future prospects are summarized in section 10.

2. Experiment Objectives

[6] The HIRDLS team's starting point was the recognition that previous satellite experiments had successfully observed dynamical and chemical phenomena in the stratosphere and above characterized by large horizontal or vertical scales. For instance, many of the research instruments that flew on the Nimbus series of satellites or the Upper Atmosphere Research Satellite (UARS) were limb viewers that provided higher vertical resolution (e.g., Limb Radiance Inversion Radiometer (LRIR) [*Gille et al.*, 1980], Limb Infrared Monitor of the Stratosphere (LIMS) [*Gille and Russell*, 1984] or Improved Stratosphere and Mesosphere Sounder (ISAMS) [*Taylor et al.*, 1993]), but had longitudinal resolution limited to the orbital spacing of $\sim 25^{\circ}$, and also had short lives. Conversely, operational temperature sounders of that era had a horizontal resolution of several tens of kilometers, but their vertical resolution was only of the order of a scale height ($\sim$7 km) or greater. (Since that time, the Atmospheric Infrared Sounder (AIRS) on Aqua has obtained vertical resolution of $\sim$1 km in the troposphere, but increasing to 3 km from 300 to 30 hPa, and 5 km from 30 to 1 mbar [*Susskind et al.*, 2003]). Scientific attention has recently put emphasis on the many processes taking place on smaller scales.

[7] In addition, while these earlier limb sounders provided information above $\sim$20 km, in general they did not provide detailed observations of the region around the tropopause. Thus, while there was considerable information on larger-scale motions in the middle stratosphere, there was a dearth of long-term data with high vertical and horizontal resolution on dynamics and chemical composition around the tropopause. HIRDLS was designed in part to address this need.

[8] HIRDLS objectives were focused on these areas: (1) small-scale dynamics and transports, including stratosphere-troposphere exchange, polar vortex filamentation, and tropical barrier leakage; (2) upper troposphere/lower stratosphere (UT/LS) chemistry, including the measurement of species involved in the chemistry of ozone and its destruction, radiatively active species, and long-lived species that serve as tracers of atmospheric motions; (3) aerosol and cloud amounts, distributions and properties, including the location and heights of cirrus clouds and PSCs; and (4) gravity waves, including sources, distributions, wavelengths, and their roles in atmospheric dynamics. As such, these support the goals of the Aura satellite, which are to determine whether ozone is recovering as expected, how the climate may be changing, and the evolution of air quality.

3. Instrument Overview

[9] The technique of infrared limb scanning was proposed to address these questions. In this method, introduced by *Gille and House* [1971], the radiance emitted by the atmosphere observed at the horizon or limb is measured as a function of relative altitude. An algorithm processes the radiances to retrieve temperature and trace constituents as a function of pressure, incorporating the hydrostatic relation-

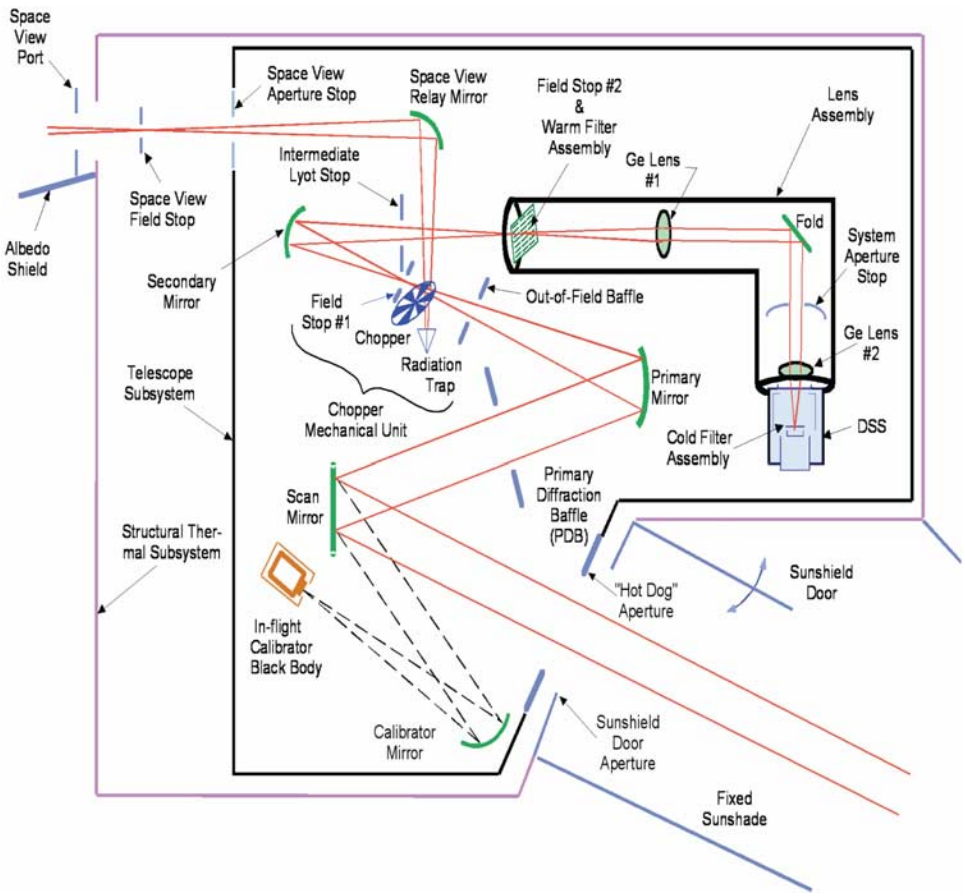

Figure 1. Optical schematic of the HIRDLS instrument.

ship, over the range of altitudes for which there is a good signal-to-noise ratio, but for which the signal has not saturated. *Gille and Russell* [1984] and *Taylor et al.* [1993] have described earlier experiments. A major advance planned for HIRDLS was the performance of vertical scans at several azimuths from the spacecraft (S/C) velocity vector, to enhance longitudinal resolution. *Gille and Barnett* [1992] gave an early description of the HIRDLS experiment. In the following sections we give a brief overview of the instrument in order to allow understanding of the problems that subsequently ensued, and characteristics of the resulting data. *Gille et al.* [2003] present a brief updated description. A more complete treatment is planned for the future.

[10] Figure 1 presents a schematic of the optical train. Radiance from the selected altitude and azimuth at the Earth's limb enters through the aperture, which is wide enough to allow scanning in azimuth from 21° toward the Sun from the rearward orbital plane to 47° on the anti-Sun side. The radiance is directed by the scan mirror to a primary mirror, which brings it to a focus where it is chopped against a reference of cold space. The radiance is recollected by the secondary mirror, and directed by a folding mirror to spectral band-defining filters, 2 lenses, then through a second set of filters (to suppress stray light) to the detectors, which are mounted on a heat-conducting sapphire rod sealed in a dewar. The cold tip of the cooler (not shown) is connected to the sapphire rod by a flexible link to prevent cooler vibration from affecting the detectors. The flex link is in a vacuum housing that can be evacuated to allow full operation in ambient conditions on the ground. HIRDLS improvements on previous limb scanners, which also are often areas of the most demanding requirements, are listed here.

3.1. Number of Channels

[11] HIRDLS has 21 channels, which confer on it several advantages over earlier limb scanners, at the expense of a large and complex focal plane. It permits more species to be measured, and thus provides better constraints on chemical reaction chains as well as providing the distributions of gases important to Earth's radiative balance. It also allows more channels to be devoted to gases whose signals in the center of their bands saturate at low altitudes. Adding channels in the more transparent band wings allows lower altitudes, including the upper troposphere/lower stratosphere (UT/LS) region, to be sounded. In addition, channels with minimal absorption by atmospheric gases can be used to observe particulates, such as clouds and aerosols. Finally, more channels can be devoted to temperature sounding, which not only provides some redundancy in case of a failure, but also yields better results. The channels and their purposes are listed in Table 1. *Edwards et al.* [1995] describe the channel selection process.

Table 1. Spectral Channels

Channel	Purpose	Spectral Band Pass (Half-Maximum Points, cm^{-1})
1	N_2O, aerosol	566.9–584.3
2	temperature	599.8–615.1
3	temperature	612.1–636.5
4	temperature	629.4–652.7
5	temperature	657.1–680.8
6	aerosol	819.9–834.9
7	$CFCl_3$	834.6–850.7
8	HNO_3	862.0–900.9
9	CF_2Cl_2	915.6–932.0
10	O_3	991.8–1008.5
11	O_3	1013.7–1044.0
12	O_3	1120.5–1139.7
13	aerosol	1202.6–1221.4
14	N_2O_5	1230.5–1257.7
15	N_2O	1255.9–1278.5
16	$ClONO_2$	1279.2–1299.5
17	CH_4	1327.0–1366.0
18	H_2O	1387.0–1432.2
19	aerosol	1401.4–1415.5
21	NO_2	1585.2–1632.9

3.2. Vertical Resolution

[12] This is improved by making use of a vertically thin detector that subtends ~1.2 km at the limb for the temperature and most other channels (channels 18 and 20 are only ~0.9 km high). The channels are arranged in 3 columns of 7 detectors each. The images of the detectors are nominally 9 km apart, center-to-center, at the limb so the total vertical height of a column is 55 km at the limb. Each detector subtends 10 km in width at the limb. With the space between the detector columns, the width of the total field of view (FOV) is also 55 km.

3.3. Lower Noise

[13] The small vertical dimension results in low signals, making low noise a prerequisite to useful retrievals. HIRDLS employs photoconductive mercury-cadmium-telluride (HgCdTe) detectors with very low noise (specified to be a few times 10^{-4} W/m^{2}sr, depending on channel). This is to be compared to signal magnitudes of order 0.1–1 W/m^{2}sr. The low noise reduces the random errors of the retrievals, as well as allowing weak signals to be seen to higher altitudes, extending the vertical retrieval range at the top and even at the bottom. It also allows signals vertically close together to be distinguished. Moreover, by oversampling by a factor of 4 or 5, with the low noise, a resolution <1 km is possible by deconvolving the radiance profiles in the manner described by *Bailey and Gille* [1986].

3.4. Precision Relative Pointing

[14] *Gille and House* [1971] pointed out that the relative spacing between radiance samples was crucial to the retrieval of temperature as a function of pressure, although absolute pointing is much less critical. HIRDLS addressed this in three ways. First, the temperature channels were located one above the other in the central column of the focal plane. In this position, any sensitivity to S/C or instrument alignment is minimized. The dimensions of the focal plane are stable, especially since it is kept at a constant temperature. The temperature channels, projected to the limb, are vertically separated by a nominal 9 km, but the actual separation was measured to an accuracy of 5 m [*Moorhouse et al.*, 2003] during calibration, better than the required 15 m.

[15] Second, HIRDLS employs another technical advance, an extremely accurate and precise encoder on the vertical scan axis, meaning that all the radiance samples are spaced very uniformly (±5 m at the limb). Given the vertical radiance gradients, this gives an uncertainty in the radiances that varies with altitude, but overall is comparable to noise, so that neither source dominates.

[16] A third possible source of pointing error is due to uncorrected rotation of the S/C around the scan axis. We have used the S/C pointing information, which incorporates information from the S/C inertial reference unit, with no additional corrections.

[17] To guard against the possibility that S/C disturbances might cause rotational motions too fast to be picked up by its attitude information, HIRDLS includes 4 gyros, allowing redundant measurements of S/C motion around 3 axes. To date this information has not been incorporated in the data processing.

3.5. Mechanical Cooler for Long Life

[18] Early limb scanners used solid cryogens to maintain the detectors at ~62 K, which is necessary for their low noise performance, especially at the long wavelengths. The ISAMS instrument on UARS had a Stirling cooler [*Taylor et al.*, 1993], but failed early for other reasons. HIRDLS was also designed with a split-cycle Stirling cooler for at least a 5 year design life.

3.6. Reduction of Scattered Radiation

[19] Because of the desire to view high altitudes and measure small signals within a few degrees of the bright lower atmosphere, extensive efforts were made to add baffles and two sets of filters to reduce stray light and ghosting. In addition, great stress was placed on optical cleanliness, to avoid scatter by particulates on the mirrors. To minimize the danger of rapidly moving debris in orbit hitting the scan mirror, HIRDLS was designed to be mounted facing rearward on the S/C. This meant that as the orbit went across the pole in the Northern Hemisphere, the aperture was pointing in the direction of the Sun. Fixed and moving Sun shields were installed to prevent sunlight from entering the aperture.

3.7. Radiometric Accuracy

[20] Radiometric accuracy was required to be ≤0.5% for the temperature channels (1% for the other channels). This placed very tight requirements on the instrument design, and especially on the entire calibration, including the blackbody targets, as well as the determination of the normalized shapes of both the FOV and spectral response functions to 1%. *Barnett et al.* [2003] gives an overview of the calibration, in a facility at Oxford University built for the purpose [*Hepplewhite et al.*, 2003]. By clever design of the facility and use of remote actuators, it was only necessary to open the vacuum chamber once, and the complete calibration, including some preliminary data evaluation, took place in less than 3 months. All the requirements on the radiometric, spectral and spatial calibration

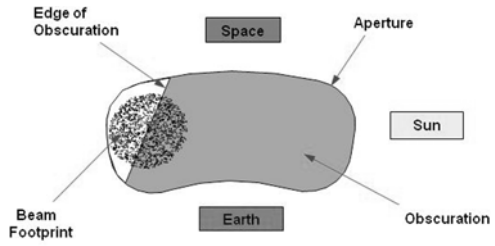

Figure 2. Schematic of aperture obscuration. The outer edge of the irregular "hot dog" shape is the edge of the aperture. Gray shading indicates approximate region blocked by the obscuration. Only area open to external view is at the extreme azimuth away from the Sun, but it is not wide enough to accommodate a complete beam width at any elevation and is narrower at the Earth side.

were met [*Eden et al.*, 2003a, 2003b, 2005a, 2005b; *Moorhouse et al.*, 2003; T. D. Eden et al., Radiometric calibration of the HIRDLS flight instrument from pre-launch calibration data, manuscript in preparation, 2008a].

4. HIRDLS Launch Accident and Effects on Coverage

[21] HIRDLS was launched on the Aura S/C on 15 July 2004 from the Western Test Range into a 705 km Sun-synchronous orbit. After 24 days for outgassing from the instrument and satellite, the coolers were gradually turned on during the evening of 9 August, and reached the 62 K detector operating temperature early on 10 August. At this point the Sun shield door was opened, and the scan mirror was commanded to perform an exploratory scan across the entrance aperture, including the atmosphere, for ~10 min.

[22] The first measurements were much different from what was expected. The radiance signal was much larger, and was much more vertically uniform than expected from the atmosphere and space. There was a region at the azimuth furthest from the Sun and orbit plane where the signal was a bit lower, and had more vertical variation. Clearly there had been a serious malfunction.

[23] The HIRDLS team, working with a NASA review board, established that an obstruction in the optics was blocking the view from the scan mirror to the aperture, as well as the view to the in-flight blackbody calibration target (IFC), preventing radiance from outside the aperture or the IFC, from reaching the detectors. Subsequent attempts to understand and simulate what happened suggest that there was air between the 2 layers of a plastic (Kapton®) film used to line the optical cavity to maintain cleanliness. During the depressurization at launch these layers could have separated, with the inner one contacting and being punctured by a sharp feature on the back of the scan mirror. Once cut, a tear in the plastic could propagate very rapidly, thus creating a flap from the inner layer. The force on it during the maximum acceleration of the launch rocket could have pulled it in front of the scan mirror. Efforts to move the blockage by various motions of the scan mirror were not successful.

[24] Scans in azimuth confirmed that at the azimuths furthest from the orbital plane there was a partial view out past the blockage. The situation is indicated schematically in Figure 2. This illustrates several key things that have been established. The blockage covers most of the aperture, with the only clear area being at azimuths furthest from the Sun, or furthest left when looking backward along the orbit.

[25] The most definitive effect of the blockage is the effect on horizontal coverage. Useful scans can only be made at the largest view angle away from the Sun, or a line of sight (LOS) of 47° on the anti-Sun side of the orbital plane, looking backward. Figure 3 makes clear the three effects this has on the coverage. Most obviously, it limits longitudinal resolution to the orbital spacing of 24.72°. Second, it prevents coverage south of 65°S, or north of 82°N, (resulting in global coverage similar to that of LIMS [*Gille and Russell*, 1984]). Finally, it precludes simultaneous measurements with other Aura or A-Train instruments at nearly the same time. Some locations can be seen on a preceding or following orbit, however. The next section addresses the question of whether the atmospheric signals seen through the partial opening at the extreme azimuth can yield useful scientific data.

5. Algorithms for the Recovery of Radiometric Data

5.1. Introduction

[26] The losses of coverage are clearly losses of capability from which there does not appear to be any recovery. However, there is some recovery from the radiometric effects of the obscuration. The partial blocking of all beams means that the signals from the atmosphere are reduced, correspondingly reducing the signal-to-noise ratio (S/N), and at the very least reducing the altitudes to which useful results can be obtained. In this section we provide a brief overview of the methods developed to recover some of these measurement capabilities. A measure of their validity will be shown by the results for temperature, contained in section 6.

[27] Henceforth, any reference to scans should be understood to be vertical scans only, at the azimuth LOS angle of −47° from the plane containing the negative velocity vector. As illustrated in Figure 2, the beams from all detectors are out of focus at this position, and are much larger than the opening at any elevation including the "space view" where the opening is largest. Thus, at any elevation angle there is signal from the obstruction, the sum of what it reflects from the interior of the instrument and what it emits at its own temperature. At the upper end only space can be observed through the opening, and the entire signal comes from the blockage. At the earthward end of the scan the atmospheric signal is added to the blockage signal. Thus, on a downward scan the signal will increase as more blockage is seen, then increase further and more rapidly as the atmospheric signal comes into view. In addition, motion of the scan mirror causes the blockage to vibrate, resulting in an oscillatory component of the signal.

[28] In order to provide an explanation of some of the characteristics of the HIRDLS retrievals of temperature and trace species, we provide a brief outline of the algorithms that have been developed to correct for the effects of the blockage. Full details will be presented elsewhere.

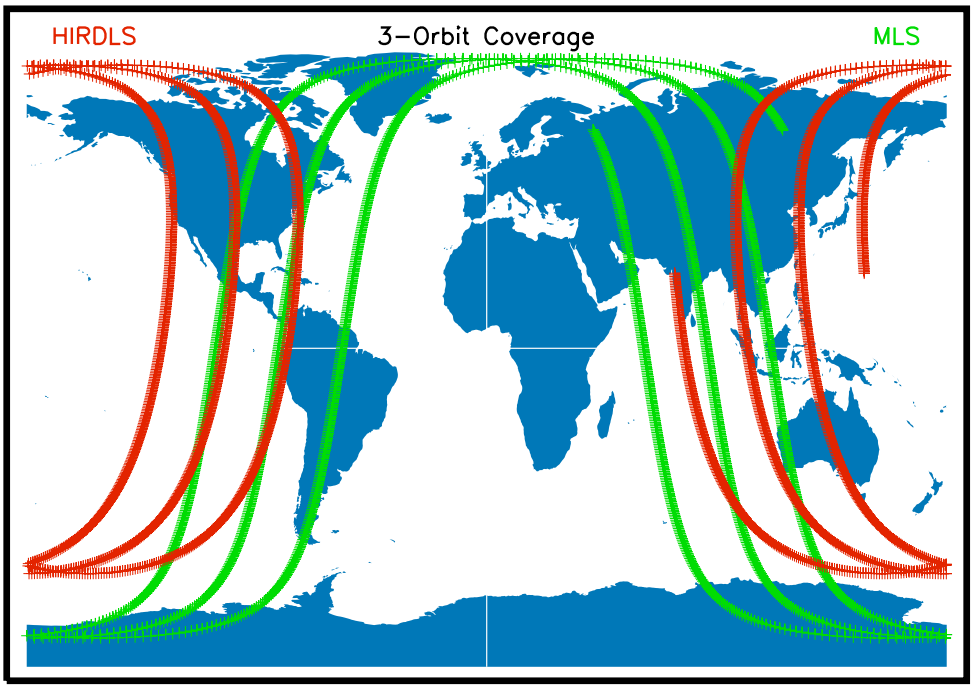

Figure 3. Coverage of postlaunch HIRDLS instrument (red), showing three orbits. The view is at a line of sight angle 47° from the negative velocity vector, on the side away from the Sun. The large azimuth angle precludes simultaneous observations of the same locations with other Aura or A-Train sounders viewing in the orbital plane. As an example, the comparison to the MLS scan track (green), in the plane of the Aura orbit, shows it viewing near same region in midlatitudes of the descending portion of the orbit as HIRDLS on the preceding orbit. On the ascending portion of the orbit the HIRDLS scan track lies between MLS scan tracks for the previous and the same orbit.

5.2. Strategy for Dealing With the Blockage

[29] At the top level, the approach is to correct the incoming signals to provide radiances as close as possible to those from an unobstructed instrument. This requires that the signals first be converted to calibrated radiances, representing the signals from the atmosphere or space in the open area plus the signal from the blockage. The next steps are illustrated in Figure 4 where Figure 4a indicates channel 3 calibrated radiances from a scan when the S/C is in its normal Earth-viewing orientation (NO), plotted as a function of the mirror elevation shaft angle. (HIRDLS convention is to measure elevation angles positive toward the Earth.) The upper portion is a view to space. Scanning downward, around −0.3° some atmospheric signal begins to be seen, followed by a steady and steeper rise, continuing to the bottom, with a notch near +0.2° due to the cold tropical tropopause. Channel 3 is sufficiently opaque at the lower levels that no variable cloud signals are seen. The oscillation can just barely be seen in the signal.

[30] In Figure 4b the oscillation has been removed, leaving the signal from the blockage plus atmosphere, denoted R. Next the estimated radiance from the blockage, termed R_S, the radiance when there is only space in the opening, is estimated and subtracted, leaving just the atmospheric component. Since this is only from the unobstructed part of the beam, it must be divided by D, the fractional open area (FOA) (Figure 4c), to obtain a full beam radiance. The final corrected radiance is thus $R_C = (R - R_S)/D$. These corrections are outlined below.

5.3. Calibration

[31] To maintain the radiometric accuracy in orbit, it was planned to view space at the upper ends of the limb scans, determining the radiometric offset on each scan for each channel. Once a minute the scan mirror was to be turned to view the IFC by way of the IFC mirror; the difference between this and the offset measurement leads to the gain. To convert the measured signals to radiances, it is necessary to apply the calibration equation [*Eden et al.*, 2005b]

$$R = B_{IFC}/(S_{IFC} - S_0)\{(S - S_0)[1 + k(S - S_0)]\}$$

where S are the measured signals, with subscripts 0 and IFC indicating views to space and the IFC, whose blackbody radiance is B_{IFC}, and k is the quadratic term determined during calibration.

[32] Since neither a view to space nor the IFC is possible, another approach had to be developed. Data taken during ground calibration at Oxford, when HIRDLS was viewing a liquid nitrogen target, showed that the space view signal S_0 could be calculated to 1–5 counts from the temperatures of the 4 reflecting surfaces (primary, secondary, back of chopper blade, and space view mirror) in the optical path (Eden et al., manuscript in preparation, 2008a). Since the full range signals are set to ≥40,000 counts, this is a negligible contribution to the error.

[33] In orbit S_{IFC} cannot be measured, but the quantity $B_{IFC}/(S_{IFC} - S_0)$ is the gain G of the system, which was determined as a function of the detector temperature T_D

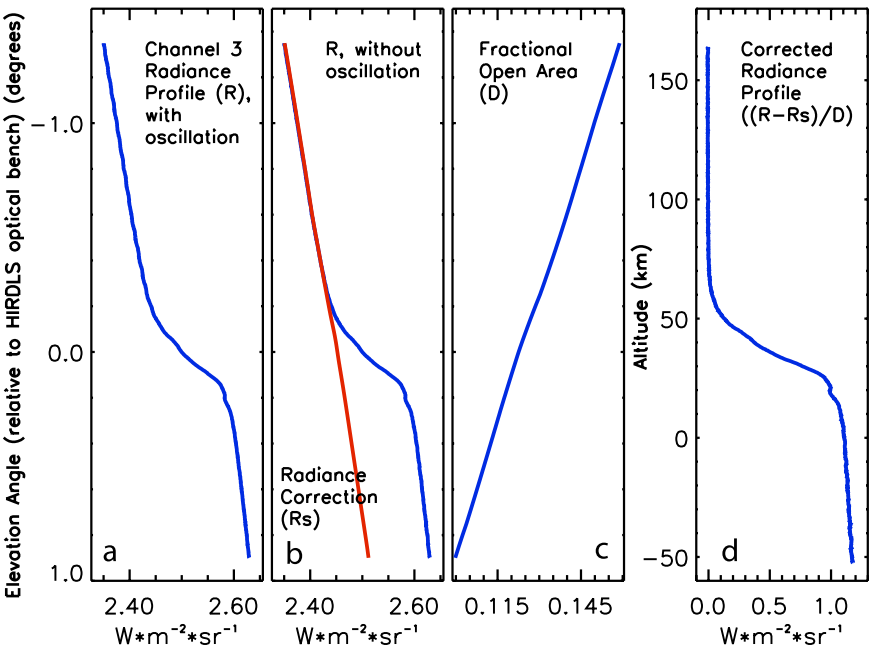

Figure 4. Sequence of correction steps. (a) Measured radiance R as a function of scan elevation angle for channel 3 scan, with oscillation present and notch for tropical tropopause; (b) measured radiance R after oscillation has been removed, juxtaposed with estimate of contribution from the blockage (R_s); (c) fractional open area (FOA) as a function of elevation angle for channel 3; and (d) corrected radiance, where R_s has been subtracted from R and divided by fractional open area D to reconstruct estimate of radiance that would be seen without the blockage.

during calibration to 0.1% [*Eden et al.*, 2005b, also manuscript in preparation, 2008a]. During calibration T_D averaged 61.632 K, although its temperature had small variations. In orbit the HIRDLS detectors have been held at 61.657 K, to within 0.001 K ± 0.001 K over almost 3 years. The gains at this temperature were determined to differ negligibly from the values obtained during calibration, and were fixed at the calibration value. Although this is unconventional, no gain change is apparent in HIRDLS observations since launch. This is continuously monitored by calculating time series of zonal mean radiances in the tropics. The noise levels, also temperature and gain sensitive, are very close to the prelaunch values, (and well below the specification).

[34] In support of this approach, the photoconductive detectors used by the AIRS are of the same type and manufacturer as the HIRDLS detectors. The AIRS detector gains have been constant to 1/4% over 5 years in orbit, and that change is believed to be due to optical degradation (D. Elliott, private communication, 2007).

5.4. Description and Use of the Pitch Maneuver

[35] In the normal orientation of the S/C, the signal from the blockage is combined with the signal from the atmosphere. A key problem is determining the blockage signal, R_S, so it can be subtracted. As suggested by Figures 2 and 4, and the previous description, the blockage signal varies with elevation angle and with time, because of changes in instrument and blockage temperature as a function of position in orbit. An estimate of this can be obtained if the S/C performs a pitch maneuver (PM), in which the front of Aura is pitched down by 5.25° so that HIRDLS' LOS, looking out the back, is above the atmosphere for all channels. In this PM case only the blockage is seen, and the behavior of its signal can be characterized. The assumption is that the behavior does not change significantly between PM and NO, which appears to be the case. Pitching to the intermediate angle of 2.62° also allows this to be evaluated.

5.5. Removal of the Oscillation of the Radiometric Signal

[36] When the scan mirror moves, it contacts the blockage, causing it to vibrate with a sharp spectral peak near 1.9 Hz. This motion of the blockage leads to an oscillation of the signal on top of the other signals from the blockage, space and the atmosphere, extending from top to bottom of the scan. In order to make use of the signals, this oscillation must first be removed.

[37] Data obtained during PMs were crucial in determining this correction. Simple triangular filtering isolated the oscillation amplitudes, which show up clearly and unambiguously around the orbit. They are excited at certain elevation angles, termed trigger points, presumably where the contact between the mirror and the blockage occurs. (The trigger point varies systematically in a repeatable way around the orbit.) Figure 5 (left) shows the oscillations resulting from filtering 600 up scans (~3 orbits) during a PM on 13 May 2006, exposing the regularity of the oscillations in the radiometric signal. The amplitudes below the trigger point are small, but at that point the oscillations are excited, and continue for the rest of the upward scan. The

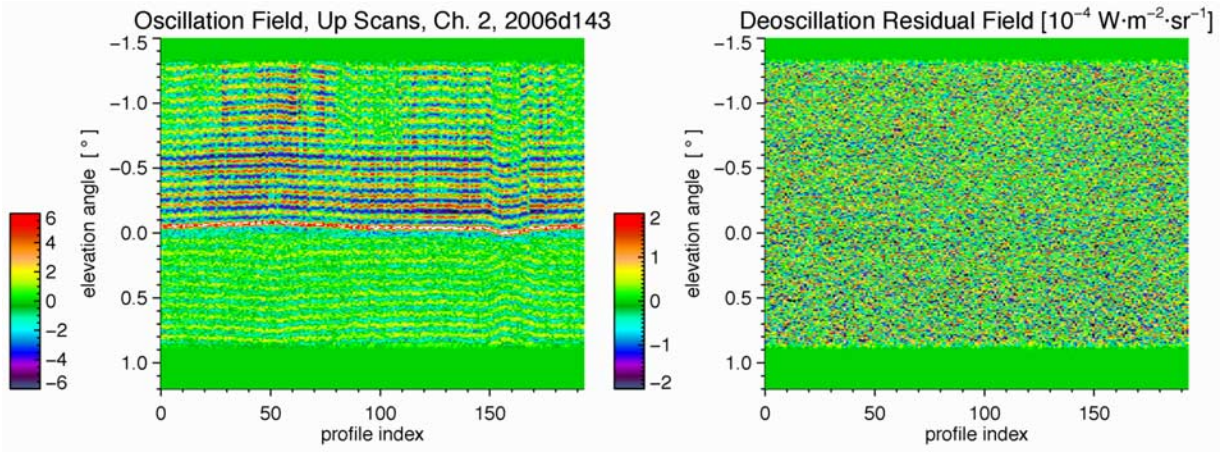

Figure 5. Six hundred up scans (three orbits) of channel 2 up scans during a pitch maneuver, filtered to show effect of blockage oscillation. (left) Before removal of oscillations. (right) Same scans, after removal of the oscillations by fitting EOFs to the space (upper) portion of the scans, as done for data taken in normal science data taking orientation. Color bar has been expanded in Figure 5 (right), showing oscillations have been completely removed and cannot be seen above noise level.

peak-peak amplitudes are $\sim 12 \bullet 10^{-4}$ W/m^{2}sr, (compared to the noise level of $\sim 1 \bullet 10^{-4}$ W/m^{2}sr).

[38] The radiometric oscillations from the PM were subjected to singular value decomposition (SVD), leading to16 empirical orthogonal functions (EOFs) spanning the whole range of elevation angles. In NO, the space view is divided into a number of elevation angle ranges, and the 16 EOFs are fit in each of them for each scan, and the oscillations are subtracted from the signal. The EOFs in the lowest angular range extend through the atmospheric region, removing the oscillation there as well. Results simulating this case are shown in Figure 5 (right), illustrating the removal of the oscillation down to the noise level. By looking at PM data it is possible to see directly what is happening at angles where the line of sight is in the atmospheric range in NO. The RMS errors passed on to the next steps are $1.795 \bullet 10^{-4}$ W/m^{2}sr, at the noise level at this stage of processing. The most stringent test is with the radiances and retrievals, which show no residual oscillation signal in the atmospheric region.

[39] The oscillations seen in the space view determine the amplitudes of the EOFs to use to remove the oscillations in the atmospheric region during NO, and do not remove (or add) atmospheric features. In particular, there is no effect of the oscillation removal on signals from gravity waves or other disturbances.

[40] After discovery that the scanner motion caused signal oscillations, tests showed that azimuth scans or faster vertical scans generated more oscillations. Four scan patterns were tried over time looking for the best combination of low oscillations and scan speeds. The scan parameters and dates are shown in Table 2. Except for a different set of EOFs to remove the oscillations, all scan patterns are subject to the same data processing, and have the same characteristics. The only difference in the data is that for scan table 30 there are slightly larger residuals of the oscillations, reaching up to twice the noise levels, for descending orbit tropical latitudes.

5.6. Determination of the Blockage Signal, R_s

[41] As noted above, the blockage in the HIRDLS optical train can emit its own radiance, and reflect radiance from the interior of the optical cavity. Observations, both in the PM position and in NO, show that this radiance, which increases earthward, varies greatly in magnitude and also somewhat in shape around the orbit, as shown for an orbit of channel 2 down scans on 13 July 2007 in PM position in Figure 6. Removing these variations with sufficient accuracy is the greatest difficulty in correcting HIRDLS data. Data from up and down scans have been analyzed separately to calculate the mean (shown by the full dashed line in Figure 6), and the departures from the mean have been subject to SVD. The first EOF primarily indicates a shift in the mean signal, the second a change of slope, and the third includes some complex shape changes. Here again, it is necessary to use the information at those angles at which the blockage signals can be seen above the atmosphere to estimate the blockage signals at atmospheric levels where it cannot be seen. This requires a careful tailoring of angles at which the estimated blockage signal is matched to the measured signal, and the use of correlations among the EOF coefficients for the different channels. Although this method is based on the single PM on 10 July 2006, and is mostly statistical, it works reasonable well for the temperature and

Table 2. Scan Tables for Scientific Data Taking

Scan Table	Dates	Line of Sight Vertical Angular Velocity (°/s)
30	21 Jan 2005 to 28 Apr 2005	0.4400
13	28 Apr 2005 to 24 Apr 2006	0.3410
22	24 Apr 2006 to 4 May 2006	0.3108
23	4 May 2006 to	0.3108

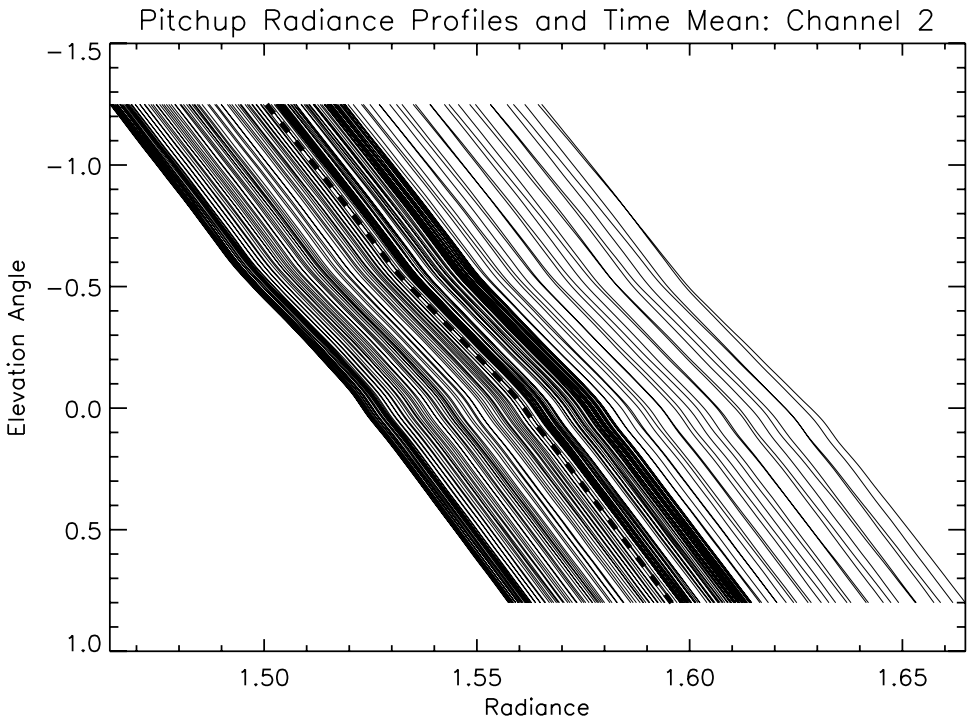

Figure 6. One orbit of channel 2 down scans at the science observation azimuth of −23.5° azimuth shaft angle during pitch maneuver. HIRDLS line of sight is up 5.25° above normal orientation, so the atmosphere is not in the line of sight. In this plot, Earth is at bottom (larger positive values of elevation angle), and space is at top (large negative values of elevation angles). Radiance increase with elevation angle primarily reflects the blockage filling an increasing fraction of the beam as scan proceeds toward Earth.

ozone channels, where the signal is large. New approaches are being developed to put this correction on a more physical and hopefully more accurate basis, in order to recover additional species. Residual errors from this step are

$$\sim \pm 10 \bullet 10^{-4}\,\mathrm{W/m^2sr}.$$

5.7. One-Time Correction for the Fractional Open Area

[42] Although the FOA is conceptually simple, its determination is not. The most reliable method appears to be to model the radiometric signal when vertically scanning over an azimuth angle viewing only the blockage, and at the science scanning azimuth of −47°, and determining the FOA from the difference (T. Eden et al., Spectral characterization of the HIRDLS flight instrument from pre-launch calibration data, manuscript in preparation, 2008b). An example, showing the magnitude and variation with elevation angle was shown in Figure 3. Work to refine these calculations continues, but at present we estimate an uncertainty of +5/−15%.

5.8. Filtering and Establishment of the Vertical Grid

[43] At this point radiometric data for all channels have been sampled at an 83 Hz rate, and reduced to a 28 Hz bandwidth by a digital finite impulse response (FIR) filter. The data still contain high frequencies that contain noise and not useful signals, so they are fast Fourier transformed, band limited at 1 cycle/2 km, and transformed back. This effectively sets the bandwidth at ∼7.5 Hz, reducing the noise by a factor of 2.

[44] The data are still on a nearly uniform grid in elevation angle, but altitudes have been assigned to each sample. These are then splined onto a uniform grid in altitude with 1 km spacing from 0 to 120 km.

5.9. Radiance Adjustment

[45] After applying these corrections, it was found that the right features were seen in the right places, but the magnitudes were generally too small. To correct this, a one-time adjustment is made to the radiances. For each of the temperature channels the expected radiances were computed for each scan for 18 May 2006. The calculations for channels 2–5 were based on the Goddard Modeling and Assimilation Office (GMAO) Earth Observing System version 5 (GEOS-5.01) meteorological data. The radiances for these channels, corrected as described above, were divided by the calculated radiances, and the ratios separated into 10° latitudinal bins for the ascending and descending parts of the orbit. On inspection, the ratios in all bins were similar. A global average radiance adjustment factor was therefore calculated, and is applied to all radiances for the entire mission as a one-time correction. This is to make up for the present imprecision of our knowledge of the FOA, and to a lesser extent our uncertainty in correcting for R_S. Each channel has a range of altitudes over which the mean radiance ratio is used directly to adjust the radiances. The

lower altitude of the ranges is 9 km for all channels. The upper altitudes for channels 2–5 are 50, 60, 60, and 65 km, respectively. The adjustment is smoothly transitioned from the ratio at the upper altitude to unity over the 15 km immediately above these upper altitudes. For the temperature channels this factor is near 10% at low altitudes for all channels. The value drops to less than 1 at roughly 50 km, and reaches 0.8 at the top of the adjustment region. Since a single factor is applied for all latitudes, there is a possibility that this could lead to variations in data quality as a function of latitude.

[46] As all corrections are better determined on a physical basis, this factor will approach 1, and become less necessary, and ideally not needed at all. At present it is a diagnostic of the state of the combined correction algorithms. It should be pointed out that this step essentially makes the biases of the HIRDLS data equal to those of the GMAO data. This adjustment is very smooth in altitude, and thus will not introduce any high frequency variations that could be mistaken for atmospheric variations. Systematic errors, including an apparent offset in pointing directions, as well as low S/N, limits this version of the temperature data to the lowest mesosphere. Future versions should extend this limit well into the mesosphere.

[47] All scans took around 15 or 16 s. For ST 23 there are about 5530 scans per day, with an along-track spacing between scans of 101 km. Note that this results in a ratio of horizontal to vertical spacing of ~100, roughly the ratio of the Brunt-Vaisala frequency to the Coriolis parameter outside the tropics, which is ideal for sampling dynamical features there [*Lindzen and Fox-Rabinovitz*, 1989].

6. Outline of the HIRDLS Temperature Retrieval Algorithm

[48] The retrieval algorithm has been described by *Lambert et al.* [1999] and by R. Khosravi et al. (Retrieval algorithm and characterization for the High Resolution Dynamics Limb Sounder (HIRDLS), manuscript in preparation, 2008). Here we briefly outline it, especially as it applies to temperature, and changes necessitated by the blockage in the optical train. The retrieval algorithm is a maximum a posteriori retrieval [*Rodgers*, 2000] of the radiances determined from channels 2–5, following the physics outlined by *Gille and House* [1971]. Input data is on a uniform altitude scale, but the solution returns temperature and pressure at these levels, with the pressure and altitude hydrostatically consistent.

[49] A key to the retrieval is the radiative transfer forward model (FM), used to calculate the atmospheric radiances rapidly and accurately for any atmospheric state. *Francis et al.* [2006] describe the development and testing of the FM, which includes allowance for the temperature variations along the LOS. Briefly, it combines physically based transmittance estimates from Curtis-Godson and Emissivity-Growth approximations in a statistical regression. Comparison against a reference model with the same accuracy as a line-by-line calculation for a set of representative atmospheres gives errors considerably better than 0.5%, and often less than 0.2% for channels 2–5 up to 100 km.

[50] The retrieval starts from an initial guess. On the basis of prelaunch tests using model data, and the averaging kernels shown in Figure 7, the retrieval algorithm is very insensitive to the choice of initial guess. It was planned to use climatology to provide the initial guess and the HIRDLS retrievals at multiple azimuths to provide information on gradients along the line of sight. As the latter is precluded by the blockage, the approach was changed to using GEOS-5 assimilated meteorological data to provide the LOS gradients, and also the first guess, as MLS does [*Schwartz et al.*, 2008]. On each iteration the temperature at the tangent point is adjusted, keeping the LOS gradient fixed.

[51] The CIRA86 climatology [*Fleming et al.*, 1990] is used for the a priori temperature, with an uncertainty of ±20 K on the diagonal of the error covariance matrix. Off-diagonal matrix elements fall off with a scale height of 5 km.

[52] The averaging kernels shown in Figure 7 for every 3rd level show the sharp peaks typical of limb scanning instruments, and have widths ~1 km. With the areas under the kernels (red line) close to 1, they also indicate that the solution will follow the radiances very closely, and thus not be sensitive to the initial guess or the a priori profile. This holds up to close to 0.1 hPa, which is the current temperature retrieval range.

[53] These expectations are supported by 2 tests. In the first, the same first guess was used for an entire day, and the results compared to those from a standard run. The RMS differences were ≤0.79 K at all levels from 16 to 54 km, with an overall RMS difference of 0.10 K, indicating minimum sensitivity to the initial guess over our main region of interest. In the second test the a priori for the initial profile was used for an entire orbit. In this case the RMS differences were less than 1 K from 16 to 54 km. The RMS over all altitudes from 9 to 69 km was 0.11 K. These results confirm that the retrievals are following the radiances.

[54] On completion of the retrieval, data are interpolated to a set of pressure levels, with 24 levels per decade of pressure, uniformly spaced in log pressure, or about 10% in pressure spacing between levels.

7. Validation of the HIRDLS Temperature Retrievals

7.1. Approach and Rationale

[55] HIRDLS temperature retrievals are critical to the experiment, since they are required for the retrievals of the HIRDLS trace gases. Temperatures also play a central role in dynamical studies, and are needed for studies of the radiative balance and chemistry. Because of the centrality of the temperature measurements, we will discuss the quality of the HIRDLS temperature results in this overview of the experiment. The comparisons are based on data processed with the V2.04.09 suite of algorithms for over 330 "days of interest" between 21 January 2005 and 15 August 2007, plus a number of additional days. These were primarily selected on the basis of the availability of correlative data for one or more HIRDLS products.

[56] The objective of this validation is to determine what biases or mean differences there may be from accepted standards, to determine any dependences of these biases on latitude or time, and to estimate the precision of these determinations. A number of comparisons are presented to

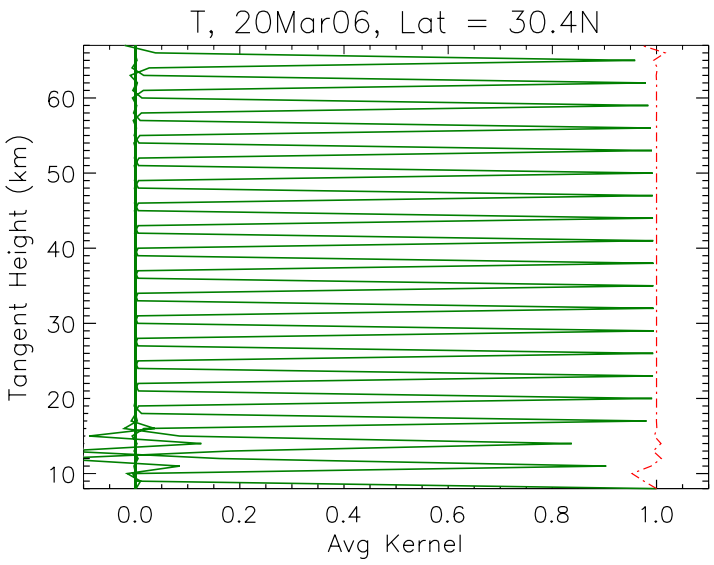

Figure 7. Averaging kernels for temperature for midlatitude equinox conditions, showing sharply peaked shape and 1.2 km. width. Every third averaging kernel is shown. Dashed line is sum of averaging kernels. Sum close to 1 indicates retrieval closely follows radiances.

evaluate systematic errors. First, a comparison with U.K. Meteorological Office high-resolution sondes (http://badc.nerc.ac.uk/data/radiosonde/radhelp.html). These maintain the vertical resolution of the original data, which allows comparisons with HIRDLS retrievals to just above 10 hPa, although in general there will be horizontal and temporal differences in the locations of the profiles that we have not attempted to remove. Next we compare with lidar data, to extend the comparisons up into the mesosphere, although at fewer locations. We also compare to ACE-FTS temperatures at high northern and southern latitudes. Finally we compare to ECMWF analyses. At lower levels these not only contain many more sondes than those mentioned above, but also satellite data from the AIRS on Aqua and others. Available 4 times per day, these are interpolated in space and time to the HIRDLS profile locations, although they have lower

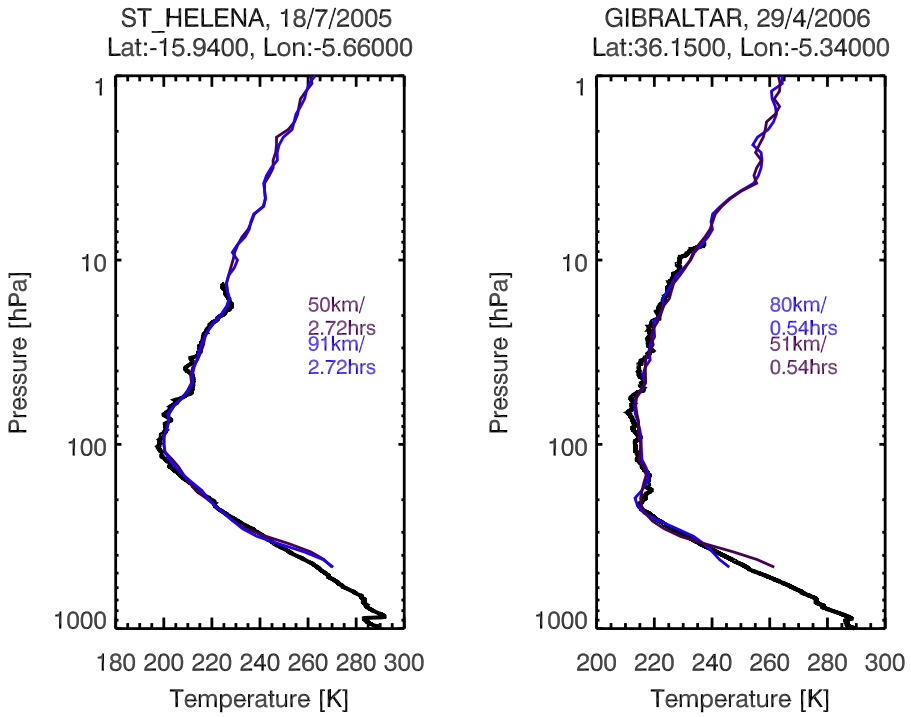

Figure 8. Pairs of HIRDLS profiles (black lines) compared to high-resolution sondes (blue and magenta) at St. Helena and Gibralter, illustrating agreement between HIRDLS retrievals and their ability to track small-scale structure in profiles above 200 hPa.

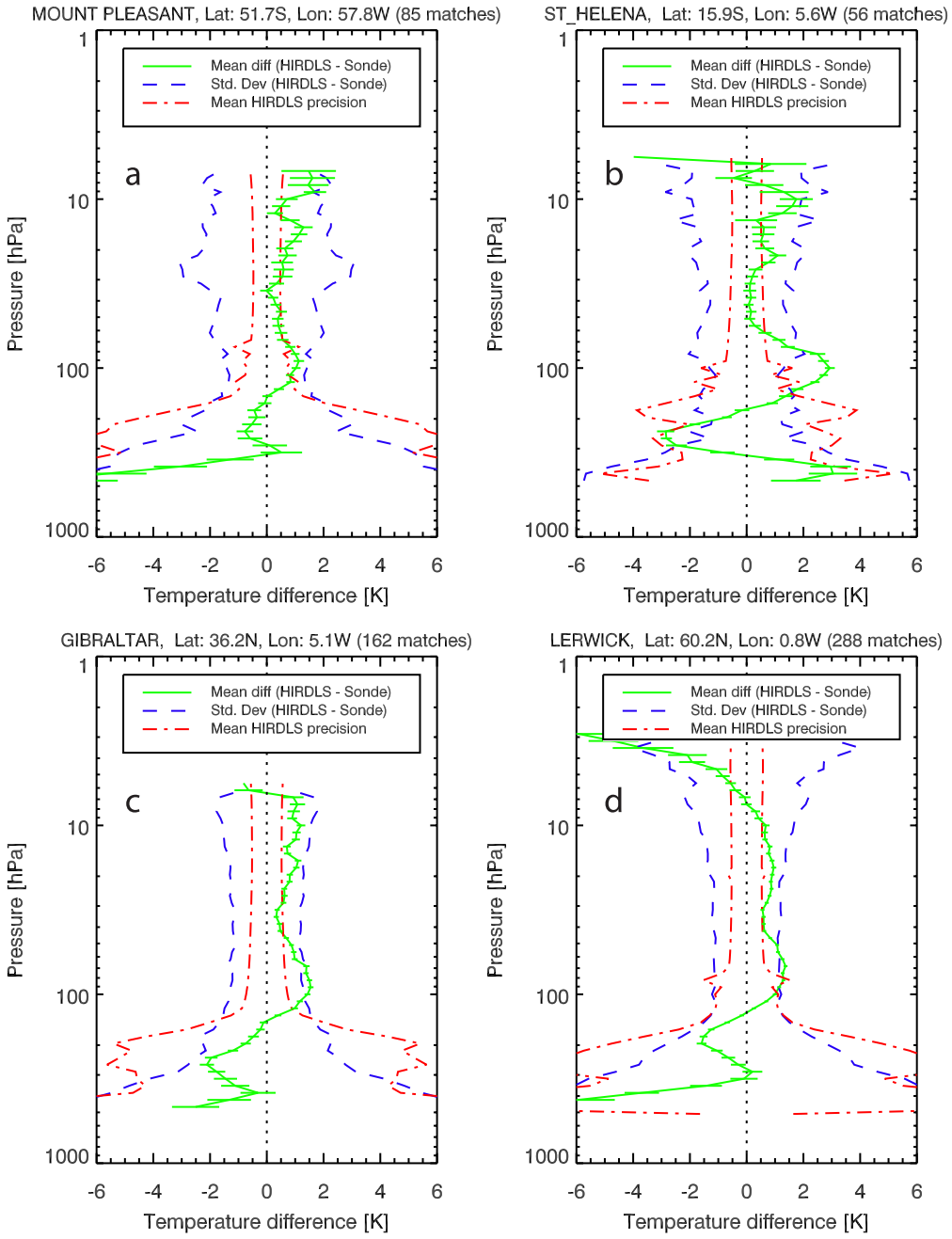

Figure 9. Statistics of HIRDLS minus sonde differences for Mt. Pleasant (Falkland Islands), St. Helena, Gibralter, and Lerwick (Scotland). Solid green lines are mean differences, with bars indicating standard error of the mean. Red dotted lines indicate HIRDLS predicted random errors, and dotted blue show standard deviations of the differences.

vertical resolution, and may have errors at the upper levels because of the lack of input data. (There are no comparisons with MIPAS data, since at this time there were very few European Space Agency (ESA) standard temperature retrievals for the HIRDLS period.)

7.2. Comparison to High-Resolution Sondes

[57] The HIRDLS temperatures were compared to U.K. Meteorological Office high-resolution data from radiosondes for 9 widely distributed stations, and for all data available from January 2005 until August 2007. Vaisala (http://www.vaisala.com/weather/products/soundingequipment/radiosondes/rs92) quotes a total uncertainty of 0.5C (95.5% confidence) in the sounding, with a precision of 0.3–0.5C from 100 to 3 hPa. Close pairs of HIRDLS retrievals are compared to individual sondes for 2 of the locations in Figure 8. The 2 HIRDLS retrievals for Gibralter, St. Helena and Lerwick (not shown) show very good agreement with the sonde and with each other. These also illustrate the fidelity with which the HIRDLS retrievals track the smaller-scale variations of the sondes above 200 hPa. However, HIRDLS

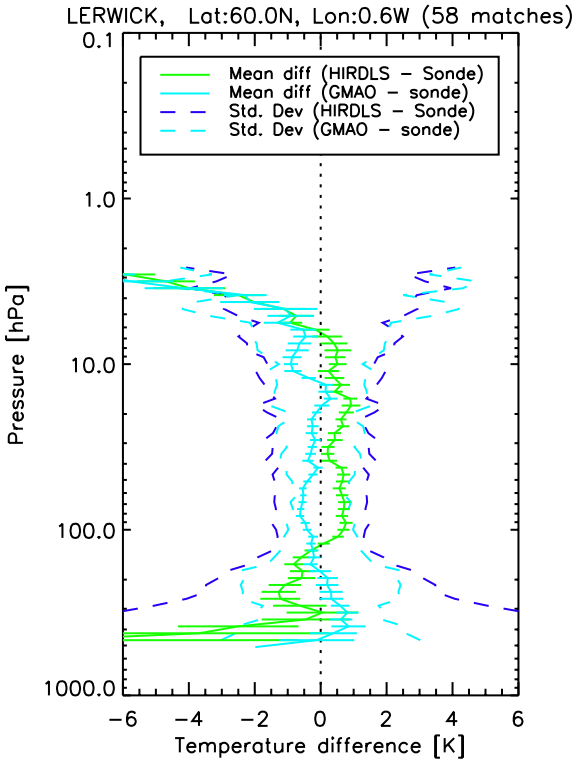

Figure 10. Comparison of mean and standard deviations of HIRDLS and GMAO with Lerwick sondes. HIRDLS and GMAO mean differences are green and light blue solid lines, respectively. HIRDLS and GMAO standard deviations dotted dark blue and light blue lines, respectively.

appears to overestimate the tropopause temperature at St. Helena.

[58] Figure 9 presents statistics for these comparisons at the 4 representative sonde locations covering a wide range of latitudes. The coincidence criteria were 300 km and 3 h (4 h for St. Helena). With one exception, HIRDLS is between 0 and 2 K warmer than the sondes between 200 and 7 hPa. Within this, HIRDLS is slightly warmer between 100 and 60 hPa, slightly cooler from 60 to 20 hPa, and warmer again around 10 hPa. The exception is the 3 K overestimate around the tropical tropopause at St. Helena. The Lerwick data, which extend higher, indicate that HIRDLS is becoming colder than the sondes above about 6 hPa, and temperatures there are cooler than the other locations at 10 hPa. Otherwise, at almost all altitudes from 200 hPa up to 7 hPa, the mean HIRDLS is within ±2 K of the sonde temperatures.

[59] Results were cited in section 6 showing the retrievals are insensitive to the initial guess. Therefore, the use of the GMAO as the initial guess will not influence the retrievals at the locations of the sondes. Figure 10 compares the mean and standard deviation (SD) of the differences between GMAO and the sondes, and HIRDLS and the sondes, for Lerwick. These results are similar to those at the other sites. Mean differences are very comparable. HIRDLS' standard deviations are slightly larger in the lower stratosphere, very comparable around 10 hPa, and lower above 5 hPa. This comparison has been extended to comparisons with lidar data in the upper stratosphere (next section), where there are fewer sources of input data to the assimilation. In these cases (not shown) the SDs of the HIRDLS and GMAO differences with the lidars are close up to 2 hPa, above which the HIRDLS-lidar differences are considerably smaller than the GMAO-lidar differences, as expected.

[60] There are two reasons why the GMAO differences may be smaller in the lower stratosphere. These sonde observations may have been assimilated by the GMAO

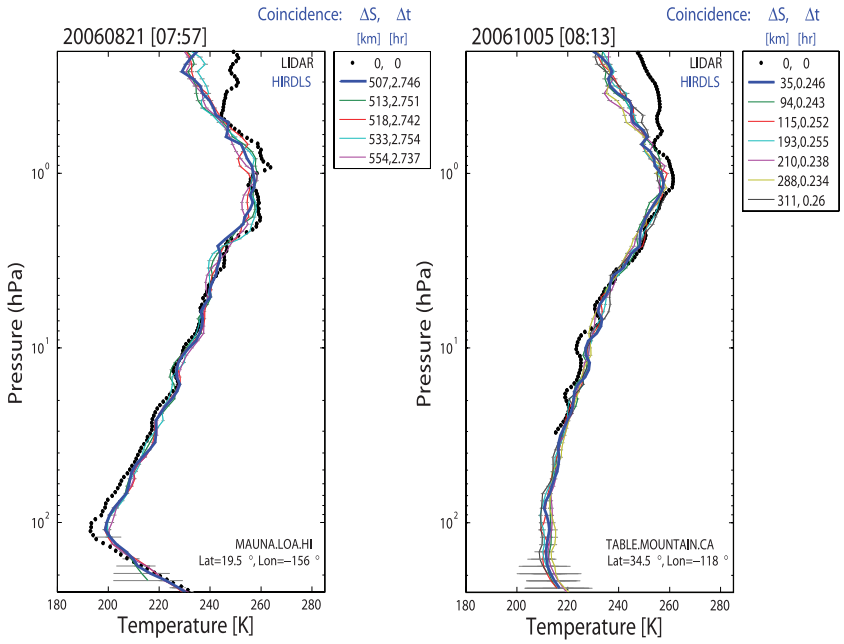

Figure 11. Representative comparisons for (left) Mauna Loa and (right) Table Mountain Observatory, showing general agreement up to the upper stratosphere, as well as ability to track small-scale features.

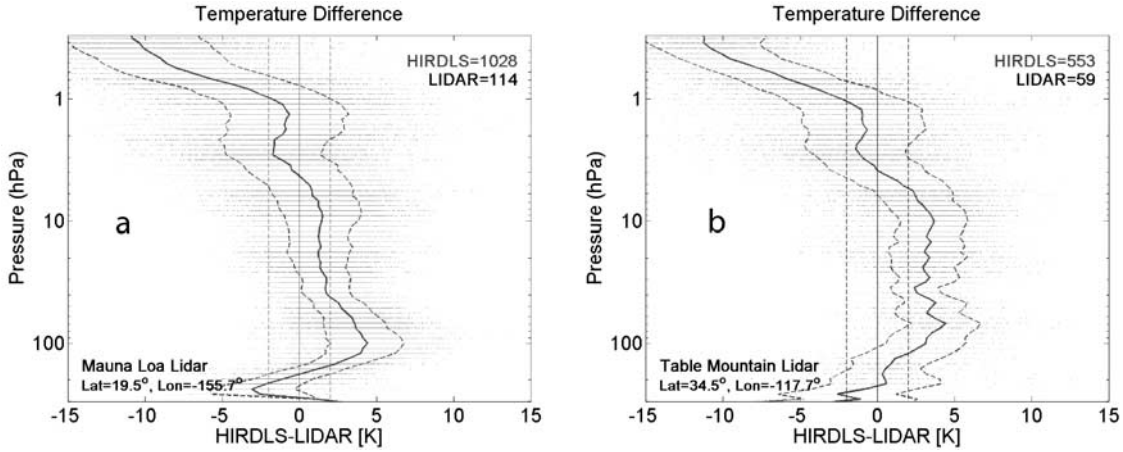

Figure 12. Statistics of HIRDLS minus lidar temperature comparisons at (left) Mauna Loa and (right) Table Mountain Facility.

analysis system, meaning that GMAO-sonde differences are a measure of the ability of the analysis to match the input observations. This could be tested by looking at data that are not ingested by the GMAO, such as the COSMIC temperatures. The second possibility is that there is so much data from all sources going into the analysis that it determines stratospheric temperatures very well at all locations.

7.3. Comparison With Lidars

[61] In order to assess bias to a higher altitude, comparisons to the Mauna Loa and Table Mountain lidars have been carried out. Figure 11 (left) shows a comparison for 21 August 2006 at Mauna Loa, where 5 HIRDLS profiles (color) are compared to the lidar (black). The closest HIRDLS profile, shown by the heavy blue line, was 507 km distant, and separated in time by 2.75 h. Here the agreement between them through the small-scale structure from 3 to 50 hPa is striking.

[62] Similarly, Figure 11 (right) shows a comparison on 5 October 2006 at Table Mountain, again showing that HIRDLS recovers the same small scales around 10 hPa, and a reasonable shape at the stratopause. Here the closest HIRDLS profile is 35 km away from the lidar, and 15 min different in time.

[63] The statistics of these comparisons is presented in Figure 12. The coincidence criteria were 560 km and 12 h, and more than one HIRDLS profile is compared with a single lidar profile. In Figure 12 (left) the statistics for Mauna Loa again indicate HIRDLS overestimates the temperature around the tropical tropopause region, here by up to ~4 K, but they agree within 2 K from 40 to 0.9 hPa. Statistics at Table Mountain (Figure 12, right) show HIRDLS warmer by about 3 K from 100 to 10 hPa, which

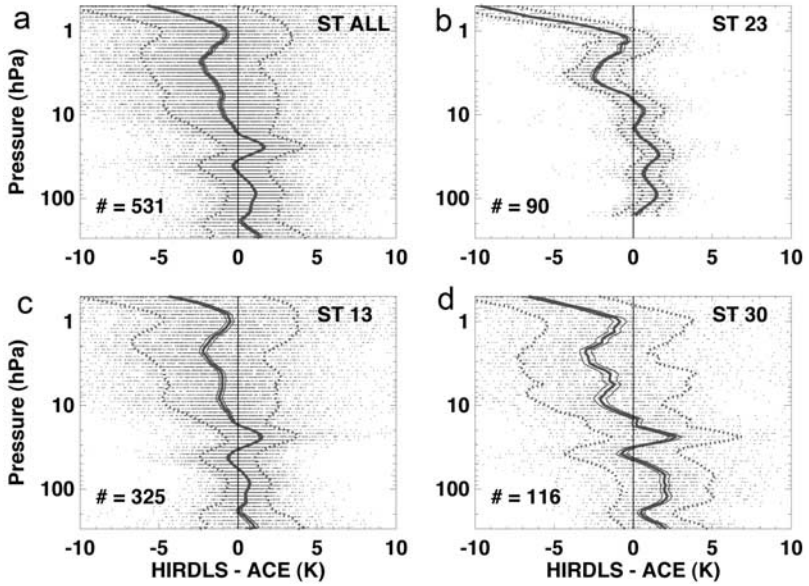

Figure 13. HIRDLS minus ACE-FTS temperature comparisons (a) for all scans and (b–d) for different scan patterns, showing means ± 1 SD. The warm feature at 23 km corresponds to a known cold artifact in the ACE-FTS temperatures [*Sica et al.*, 2007].

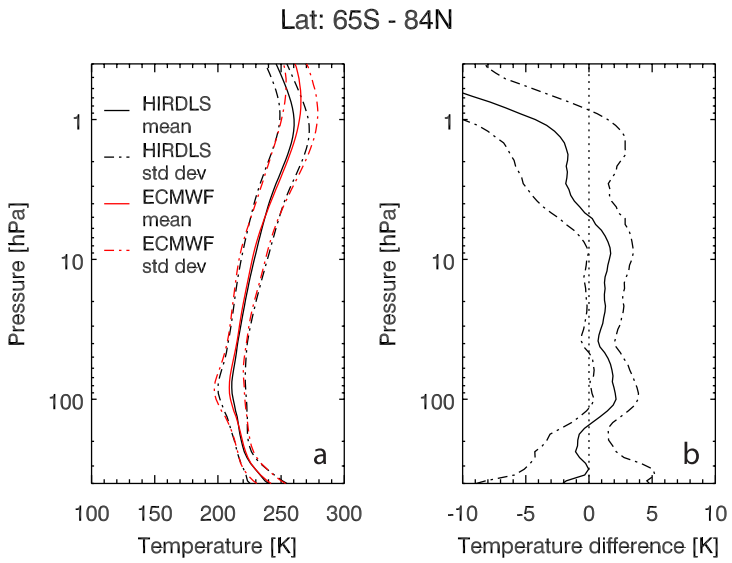

Figure 14. Comparison of HIRDLS temperatures with analyzed ECMWF temperatures interpolated to HIRDLS measurement locations. (left) Mean and standard deviations of HIRDLS and ECMWF temperatures over latitude range of HIRDLS observations and (right) HIRDLS minus ECMWF differences±1 standard deviation of the differences.

differs from zero by more than 1 SD of the differences, above which HIRDLS begins to decrease. HIRDLS is cooler than the lidars at both sites above 5 hPa.

7.4. Comparison to ACE-Fourier Transform Spectrometer Temperature Profiles

[64] HIRDLS profiles were compared to coincident retrievals of data collected by the Atmospheric Chemistry Experiment Fourier Transform Spectrometer (ACE-FTS, hereafter simply ACE) [*Bernath et al.*, 2005]. These are version 2.2 ACE temperature data, now also being validated [*Sica et al.*, 2007].

[65] Measurements corresponding to all HIRDLS scan tables were included in the comparisons presented here. HIRDLS data were omitted if the a priori contribution was larger than 30%. Because of poorly understood problems at its highest southern latitudes, resulting in increased variability, HIRDLS data poleward of 63°S were also omitted from the comparisons.

[66] Coincidences were defined as occurring within 2 h in time and 500 km. A total of 531 ACE profiles were found to be coincident with at least one HIRDLS profile, between latitudes of ~65 and 73° in the Northern Hemisphere (NH), and additional ones between 40 and 63° in the Southern Hemisphere (SH). There were often numerous HIRDLS profiles coincident with a single ACE profile, but only the comparison with the closest (in distance) HIRDLS profile is shown here. Because of their very different locations, the coincidences in the NH or SH, have been compared separately.

[67] Figure 13 displays the differences HIRDLS minus ACE, as well as the SDs of the differences, for the different scan tables in the NH. Figure 13a shows the differences for all scan tables combined. These differences are similar to those with sondes and lidars, with HIRDLS within 2 K up to 5 mbar, and generally warmer at the lower levels, but much colder above the stratopause. Figures 13b–13d display the same results for the different scan tables. All of these show very similar features, demonstrating that the retrievals are independent of the scan table used, and thus not a function of time. The positive feature in the differences near 30 hPa corresponds to the cold region in ACE retrievals near 23 km mentioned by *Sica et al.* [2007]. SH comparisons, not shown, illustrate the same features.

7.5. Comparison to ECMWF Analyzed Data

[68] The final assessment of the biases in the HIRDLS temperature data is through comparison to the analyzed temperatures developed for operational weather forecasting. These make use of large amounts of data, which are combined through a data assimilation scheme. This provides a detailed estimate of the state of the atmosphere based on both observations and model physics. As noted above, the HIRDLS retrieval uses the GMAO temperature fields as a first guess and to provide gradients along the line of sight. These should not appreciably affect the final answer, as noted above, especially in regions of low gradient. However, we have used analyzed temperatures from the European Centre for Medium-Range Weather Forecasts (ECMWF) to provide a somewhat independent comparison, although much of the same data goes into both assimilation schemes. These data cover the full altitude range of the present HIRDLS temperature retrievals. The ECMWF data are on a regular latitude/longitude/vertical grid, and available at 4 times throughout the day (0000, 0600, 1200 and 1800 UTC). It should be noted that there was an update in the analysis scheme beginning 1 February 2006 (see http://www.ecmwf.int/products/data/operational_system/evolution/evolution_2006.html).

[69] At that time the ECMWF increased the vertical resolution by increasing the number of levels to 91, and raised the model top to 0.01 hPa. They also changed, among other things, the model resolution and coefficients for the ozone chemistry scheme. Preupdate and postupdate data

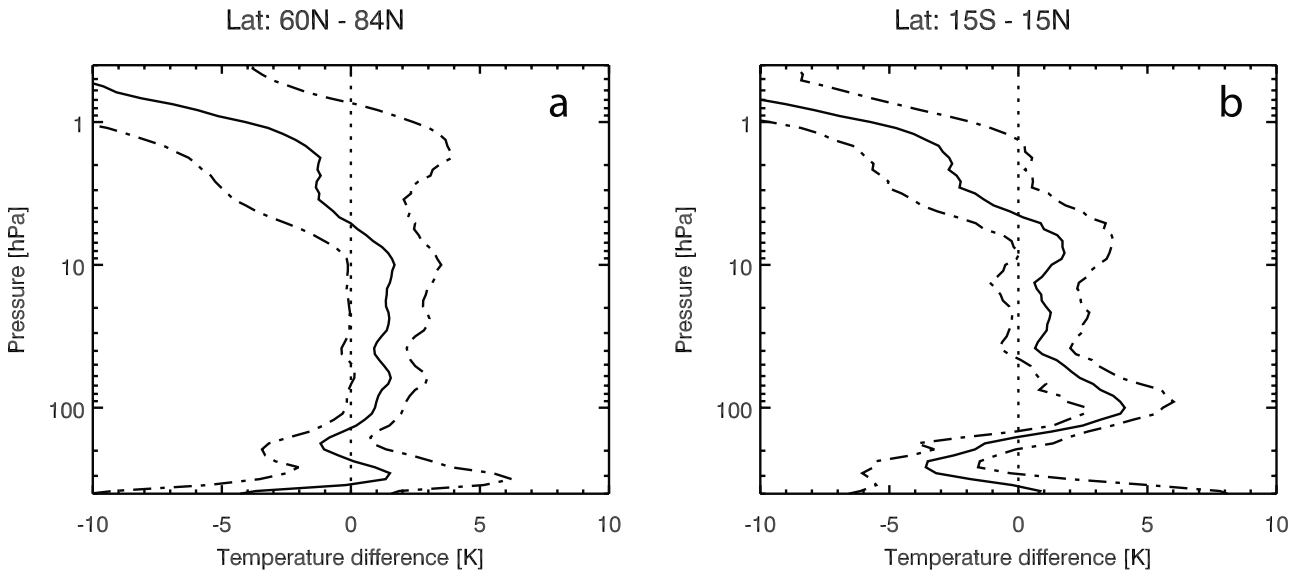

Figure 15. HIRDLS minus ECMWF temperature differences. (left) 60°N to 84° N and (right) 15°S to 15°N.

have been used together in the following analyses, as have all HIRDLS scan tables. In general, ECMWF seems to agree better with HIRDLS after the upgrade, especially at the tropical tropopause.

[70] For the following comparisons, ECMWF data are interpolated spatially and in time to the locations of HIRDLS measurements for 381 days from 23 January 2005 and 2 August 2007. Figure 14 presents a comparison of HIRDLS and ECMWF temperature profiles for the two and a half years of HIRDLS data over the range of HIRDLS latitudes. Figure 14 (left) shows the mean HIRDLS and ECMWF profiles and the profiles ±1 SD. Here the agreement is quite good on the whole, with HIRDLS slightly warmer in the lower stratosphere, and becoming several degrees cooler above 2 hPa. These differences are shown explicitly in Figure 14 (right), where HIRDLS is seen to be ~1–2 K warmer than ECMWF from 100 to 7 hPa, (with the same small variations noted in conjunction with the sondes), then becoming 1 K cooler to 2 hPa, ~4 K colder at 1hPa, and colder still above that. Overall, the two agree within ±2 K over the 400–2 hPa. pressure range. Also shown are the SDs of the HIRDLS minus ECMWF differences. The differences are within 1 SD over much of the range, but clearly the SD of the mean difference (not shown) would show HIRDLS warmer by a small but statistically significant amount. A comparison of daytime and nighttime profiles and differences (not presented) indicates that there are no significant day-night effects.

[71] Similar plots were evaluated for 6 latitude bands to ensure that these differences were representative, and that there are no large variations in the HIRDLS biases. Figure 15 (left) presents very similar results for the latitude band 60–84°N. Comparisons in other latitude bands outside the tropics (not shown) are very similar to these, confirming the pattern, and thus the absence of obvious latitudinal gradients to the biases. Figure 15 (right) shows results for the deep tropics (15°S–15°N). Again the general vertical trend is very similar, with the exception that the HIRDLS data do not capture the cold tropical tropopause, and are consistently ~4 K warmer at 100 hPa. The update to the ECMWF analysis scheme warmed the tropical tropopause by ~2 K, so the differences in the tropics are now much smaller (Figure 16, bottom).

7.6. Bias as a Function of Latitude

[72] An important question is whether these differences vary with latitude. The comparisons shown above indicate that this does not appear to be the case. Figure 16 (top) displays HIRDLS minus ECMWF differences as a function of latitude and height for November 2005 (preupgrade). The warm region around the tropical tropopause shows up as expected. There are also large differences in the polar upper stratosphere which may be due to problems with the ECMWF analysis, connected with the paucity of observational data being included there [*Simmons et al.*, 2003, 2005].

[73] Figure 16 (bottom), for August 2007, after the upgrade of the ECMWF analysis system, shows considerably smaller variations with latitude, and smaller difference with HIRDLS at the tropical tropopause. The warmer-cooler-warmer pattern from 100 to 10 hPa can also be seen. These support the conclusion that there are no large variations of HIRDLS biases with latitude.

7.7. Drift With Time

[74] Another important question, especially in view of the assumption of constancy of gain in the calibration, is whether the radiances and therefore the retrievals have drifted with time. The ACE data for the 3 scan tables shown in Figure 13 cover roughly the first 2 years of operation. They show no evidence of any significant change.

[75] Given the changes in the ECMWF analyses, the sondes are better standards against which to test for long-term changes. While there are fewer points, and significant spread in the results, the sonde system has not changed. These comparisons do not show any significant trend for any level or site. Figure 17 shows typical results, with the

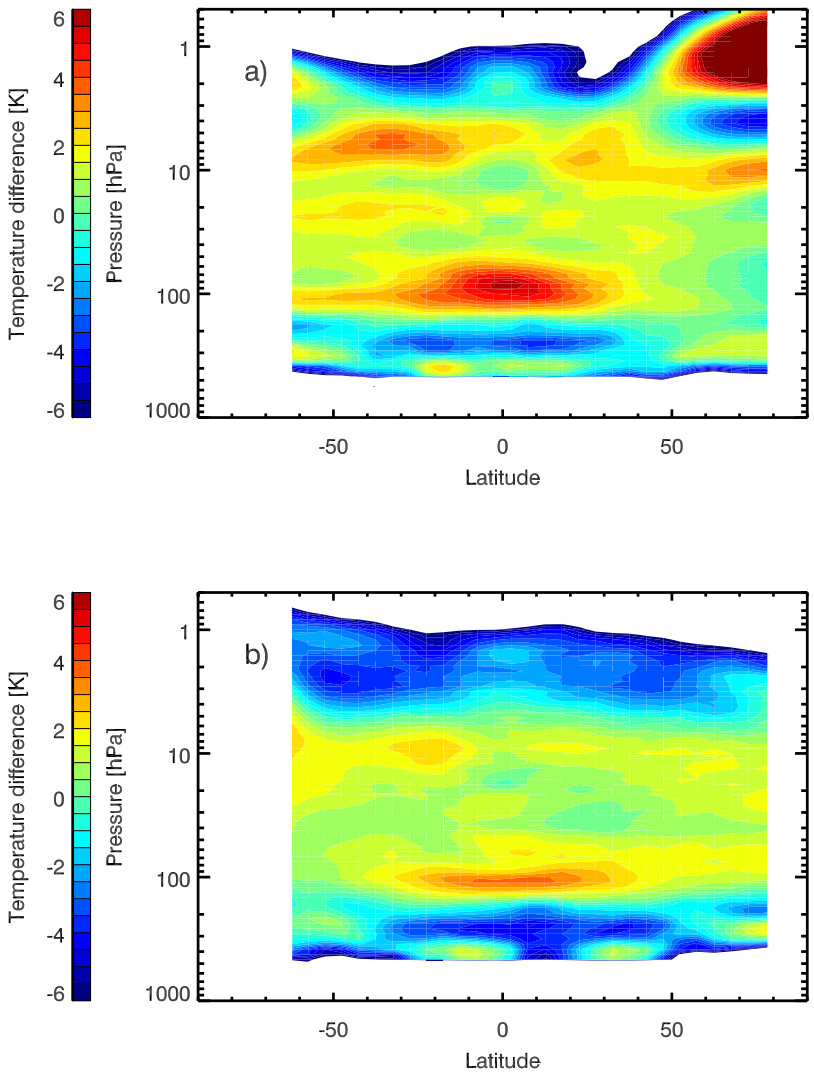

Figure 16. Plots of HIRDLS minus ECMWF as a function of latitude and altitude for (top) November 2005 and (bottom) July 2007. A large part of the change in is due to an upgrade in the ECMWF analysis system starting 1 February 2006 (see text).

temporal variation for 3 levels, for 3 different locations. The blue line is the least squares fit over the period. There is no statistically significant slope to the lines. It is clear that there is no large temporal trend to the data, (although these data cannot rule out a small drift).

7.8. Precision (Random Error)

7.8.1. Predicted Random Error

[76] In the course of the retrieval an estimate of the random error is provided, based on the measurement noise, the uncertainty of the climatological a priori information that was known before the measurements were made, FM error and the weighting functions or Jacobians of emerging radiance and temperature [*Rodgers*, 2000; *Lambert et al.*, 1999; Khosravi et al., manuscript in preparation, 2008]. The factors contributing to the random error predicted by the retrieval code are shown for a representative midlatitude atmosphere by the solid line in Figure 18. The radiometric noise of the measurement, adjusted for the reduced FOA, is not a large contributor until the mesosphere, and the a priori only contributes at the lowest levels. The primary determinant is the estimated error of 0.3% in the forward radiative transfer model. Over the region from16 to 50 km the predicted random error is 0.8 K or less.

7.8.2. Determination From Errors in Comparisons With Temperature Standards

[77] A second method, employed in the MIPAS temperature validation [*Ridolfi et al.*, 2007] is to estimate the error from the variance of the differences between the measurement being validated and the standard against which comparisons are made, minus the variance of the standard. This approach will also include the effects of differences in location and time when the measurements are made, unless special corrections are made. It will also be affected by differences in view direction for limb scanners such as HIRDLS (although we try to remove that effect by including gradient information in the retrieval), and differences in vertical resolution. In the MIPAS application, it was found that this method gave estimates of MIPAS precision that

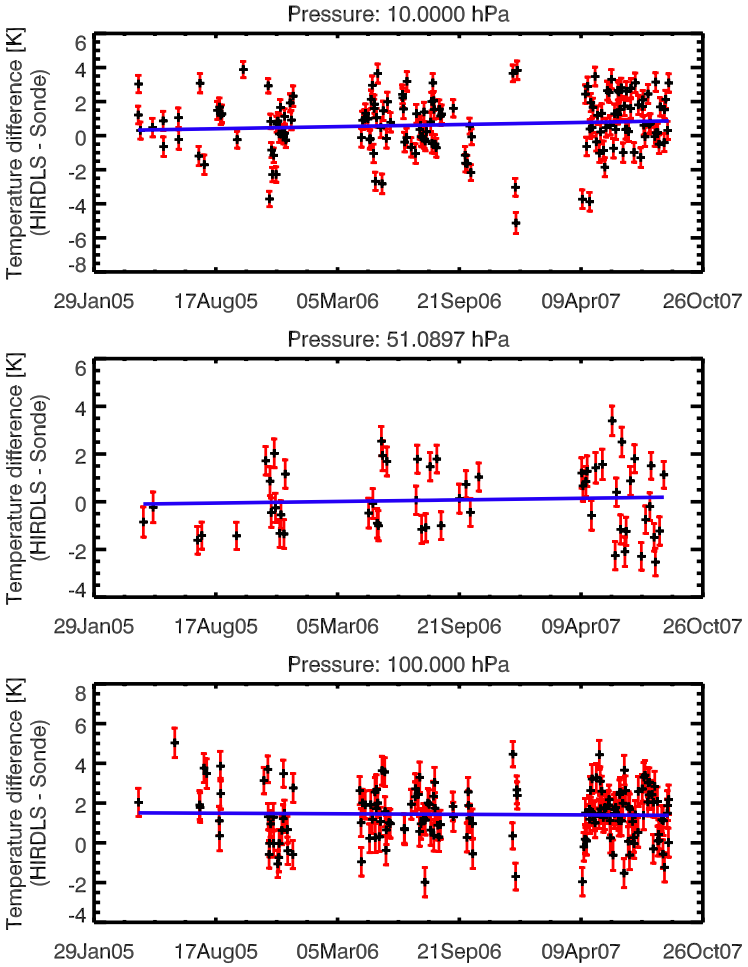

Figure 17. HIRDLS minus sonde temperatures as a function of time at (top) Lerwick, (middle) St. Helena, and (bottom) Gibralter. The blue line is a fit to the plotted values. None of the slopes are significant, indicating no a trend with time can be seen.

were a factor of 2 or more larger than expected [*Ridolfi et al.*, 2007].

[78] This method was applied to HIRDLS comparisons to sondes, and particularly the St. Helena sonde, where it was hoped the tropical location would result in smaller effects of location and remaining gradient effects. A quick calculation for 50 and 10 hPa, using a precision for the sondes of 0.1 K [*Ridolfi et al.*, 2007], implied a value for HIRDLS of 1.25°K, which is also about a factor of 2–3 larger than that shown in Figure 18. Presumably meteorological effects dominate the variance, although an underestimate of the sonde variability would have the same effect. Similarly, at 3 hPa the statistics of the differences, coupled with an estimate of up to 1 K for lidar random error [*Leblanc et al.*, 1998], implies a much larger error for HIRDLS, although here, because of many cases where the profiles were 500 km and many hours apart, it is likely that meteorological changes dominate in these cases also.

[79] As a way of avoiding many of these problems, the method was applied to the global statistics versus ECMWF at 50 hPa. Here, although the variance was smaller and the variance of the analysis was taken to be 0.5 K [*Simmons et al.*, 2005], the derived HIRDLS precision was again a factor of 2 larger than expected.

7.8.3. Comparison With HIRDLS Profiles Viewing the Same Atmosphere

[80] One definition of precision is that it is the SD of repeated measurements of the same quantity. Consistent with this, another approach to determining the precision of HIRDLS temperatures is to compare repeated views of the same atmosphere, and derive an estimate of the noise from the statistics of their differences. At 80°N and 63°S, successive scan tracks pass over the same points on the Earth's surface one orbit (99 min) apart.

[81] Results of this type of analysis are shown in Figure 19. Estimates of HIRDLS precision based on pairs of nearly coincident soundings at 63°S one orbit apart, for 3 days (~42 pairs) in each season are shown. The pairs of HIRDLS profiles are separated on average by 33 km, and meteorological changes indicated by changes in the GMAO temperatures at that location have been subtracted. The size of these depends on season: for the July case they are a few tenths of a Kelvin until reaching 1 K at 38 km, and are largest (1.4 K) at 43 km.

[82] This type of estimation also includes the effects of small-scale variations that are not resolved in the GMAO data, but change over the 99 min orbital period. They will not be eliminated by subtracting differences in colocated

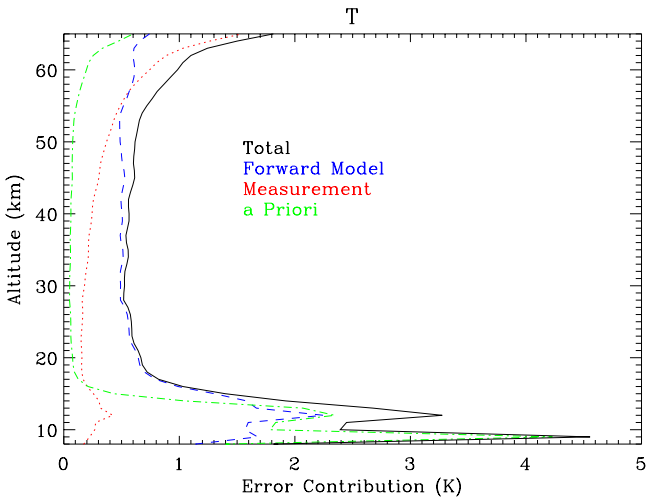

Figure 18. Components of random error calculated by the retrieval code.

GMAO profiles, and will increase the estimated precision. These estimates will thus be an upper limit to the precision. Observations in the least active seasons, when smaller-scale variations are expected to be at their minimum, are most representative. Here the values for December and March (southern summer and autumn) give results similar in shape and close to the theoretical values. The paired values below the theoretical values near 20 km may be due to use of too large an estimate of the FM error, which is smaller at low altitudes [*Francis et al.*, 2006]. This is supported by the close agreement of the empirical values derived the same way for 3 days in July in the NH up to about 40 km (not shown). The similarity between the shapes of the curves gives us confidence that the theoretical values are representative of the repeatability for slowly varying features. Conversely, estimates for the more active winter and spring cases show larger values, especially at high altitudes, as expected.

[83] The SDs of GMAO and HIRDLS temperatures for the 3 July days in 2006 are indicated by the dotted and thin solid lines, respectively. Their variations are similar in shape, although HIRDLS is larger above about 40 km. GMAO data above about 48 km are mostly model data. These curves make clear that HIRDLS precision is much less than the atmospheric variation, demonstrating that HIRDLS is able to track these variations to this level of fidelity.

8. Vertical Resolution of HIRDLS Data

[84] Establishing the vertical resolution of the HIRDLS data on a quantitative basis is not straightforward, since it is difficult to find comparative data with high vertical resolution at the same time and location as HIRDLS. The launch of the FORMOSAT-3/COSMIC constellation of 6 GPS receivers on 14 April 2006 has provided such comparative data. These enable temperatures up to the midstratosphere to be retrieved with vertical resolution of about 1 km (C. Rocken, private communication, 2007) from measurements of the occultation of the GPS signals by the atmosphere. With 1–3000 such temperature profiles being measured per day at quasi-random locations, a number of coincidences within 0.75° great circle distance and 500 s can be found with which to undertake comparisons of the two data types, including the fine vertical structure which tends to vary on a short timescale.

[85] In this study, each COSMIC profile was paired with the 1 or 2 HIRDLS profiles that fit the criteria for closeness in space and time. If there were 2, the HIRDLS profiles were averaged together. Where there were COSMIC profiles very close together in space and time, a HIRDLS profile might be used more than once in different compar-

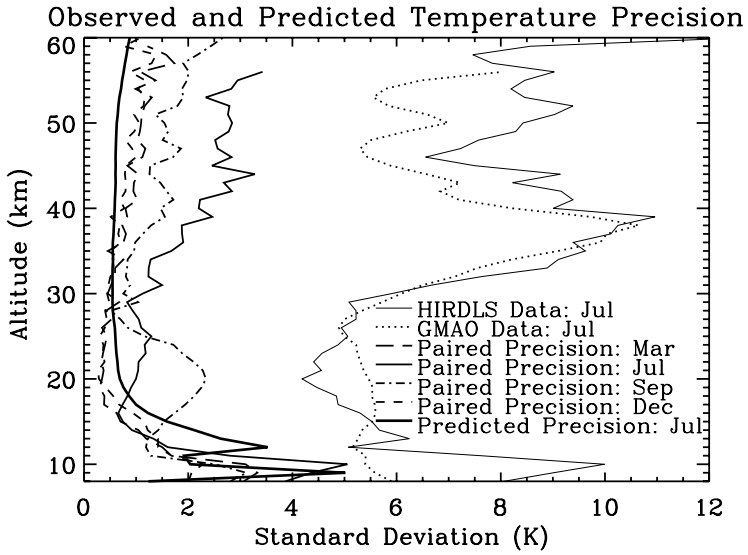

Figure 19. Empirically determined precision for HIRDLS determined from differences of paired profiles (dashed line) at latitude crossover points at 63°S for 3 days each in March, July, September, and December, compared to total precision calculated by the retrieval code (solid line). The standard deviations of the GMAO and HIRDLS data for July are also shown.

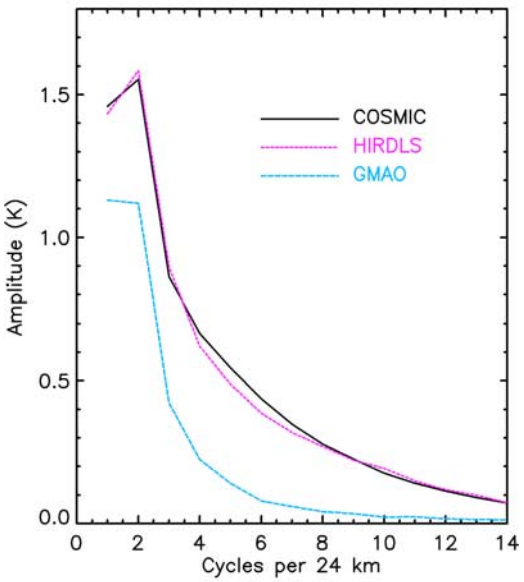

Figure 20. Spectra of temperature amplitudes versus vertical spatial frequency for HIRDLS and COSMIC retrievals and GMAO analyses. All show greater amplitudes at lower frequencies ("red spectra"), but HIRDLS and COSMIC include very similar amplitudes for higher spatial frequencies (smaller vertical wavelengths).

isons. In addition, the GMAO data were included as an indication of the short vertical scales captured by operational meteorological analyses.

[86] For this evaluation, data from 11 July 2006 to 31 October 2007 were used. The data indicate that HIRDLS is warmer than COSMIC by about 1 K from 100 to about 7 hPa. To isolate the small scales, a parabolic fit was subtracted from all 3 types of profiles over the range 2.2–5.7 scale heights, and the residual profiles then apodized. (The pressure scale height is ln 1013/p, so this corresponds to a range of 112–3.4 hPa. Since the scale height is approximately 7 km, this corresponds to an altitude range of ~24 km).

[87] When the apodized profiles are Fourier transformed, the spectra, plotted as amplitudes versus spatial frequency, are as shown in Figure 20. Here all 1217 COSMIC profiles are included, irrespective of difference of viewing directions between HIRDLS and COSMIC. As expected, the spectra all have their largest amplitudes at the lowest frequencies. The COSMIC and HIRDLS spectra are very similar for frequencies up to 12 cycles per 24 km, or a 2 km wavelength, and beyond, although the amplitudes become quite small. The HIRDLS amplitudes appear to be lower (by less than <20%) than those from COSMIC between 3 and 10 cycles/24 km, although this may be due to the spatial or temporal windows used. Figures 20 and 21 use the recently reprocessed COSMIC data. Clearly these small-scale motions are not contained in the GMAO analyses.

[88] The correlations between pairs of the profiles are presented in Figure 21. These essentially indicate the phase differences between the wave trains in the paired profiles, and show that the phase differences increase toward higher spatial frequencies. Concentrating on the HIRDLS-COSMIC correlation, this is presumably due to the more rapid changes in the smaller-scale variations, and the time differences between the observations. It does not appear to be due to differences in observation directions.

[89] This establishes that HIRDLS is capable of resolving vertical variations in the atmosphere with scales down to ~2 km. Further evaluation is continuing.

9. Discussion of Bias and Precision Estimates

[90] Summarizing the results in section 7, we see that HIRDLS is 1–2 K warmer than the sondes and COSMIC from 100 to 10 hPa. Similarly, it is ~2–3 K warmer than the lidars over this region, and warmer than ACE by the same amount, and <2 K warmer than the ECMWF analyses. There is no evidence for spurious vertical structure. The consistent result of these comparisons is that HIRDLS is warm by 1.5–2 K over this region.

[91] A deviation from this is the consistent overestimation of the temperature at the tropical tropopause, where, on the basis of sondes and the analyses, HIRDLS is 4 K warmer. However, *Borsche et al.* [2007] find that the ECMWF analyses before the update in February 2006 are ~2 K warmer than CHAMP radio occultation data. The difference is greatly reduced after the upgrade, but a large number of days from before the upgrade are included in the comparisons here. This suggests that HIRDLS may be slightly warmer at the tropical tropopause than in the rest of the lower stratosphere, but less than indicated in Figure 14

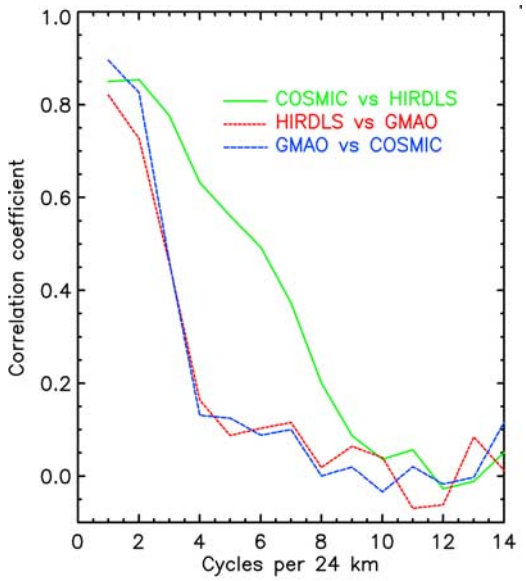

Figure 21. Correlations between pairs of vertical profiles of temperature variations from HIRDLS and COSMIC retrievals, and GMAO analyses. These indicate the phase differences between the waves in the paired profiles. The profiles could be separated by as much as 0.75° spatially and 500 s on time, and measurements were made at all relative azimuth angles. It is not surprising that these smaller scales become uncorrelated over these spatial and temporal separations.

Table 3. Summary of HIRDLS Version 2.04.09 Data Properties

Quantity	Range	Requirement
Temperatures	10–50 km	0.5–0.7 K precision, 1–2 K accuracy
O_3 mixing ratios	10–50 km (extratropics), 20–50 km (tropics)	5–10% precision, 5–10% accuracy or 0.1–0.6 ppm
HNO_3 mixing ratios	15–30 km	5–10% precision, 10–30% accuracy
Cloud top pressure	9–30 km	20%
Cloud type identification		IDs thin cirrus, PSCs, and opaque clouds
Coverage		
Vertical		10–60 km
Horizontal		65°S–82°N
Temporal		>5 years
Resolution		
Vertical		1 km
Horizontal		1° lat × 24.72° lon
Temporal		12 h (15 h revisit time in N.H.)

(right). The smaller values shown in the bottom of Figure 16 are more relevant.

[92] HIRDLS consistently falls relative to the comparison data above 10 hPa, generally becoming equal to them ~5 hPa, 2 K below around 2 hPa, and from 2 to 5 K low at 1 hPa.

[93] The warm bias for HIRDLS between 100–10 hPa, while small, appears to result from the adjustment of the radiances to match radiances calculated from the GEOS-5 temperatures. Preliminary indications are that the GEOS-5 temperatures are slightly higher than the ECMWF values [*Global Modeling and Assimilation Office*, 2007; S. Pawson, private communication, 2007]. We have not yet had the opportunity to investigate this in detail.

[94] The slightly warm temperatures at the tropical tropopause come in a difficult region, since the temperatures are low, resulting in smaller signals. There is also a dip in the averaging kernels for the tropical atmosphere. It seems likely that the combinations of the effects of low signal, noise and a priori are causing the problem. An alternate possibility is that the forward model, for some reason, is slightly less accurate under those circumstances.

[95] In contrast, the decrease in temperature above 10 hPa appears likely to be an artifact of too large an estimate of the radiance from the blockage, R_S, resulting in too low an R, or too large an estimate of the FOA (D), or both. Radiance adjustment should partly compensate for this, but this tapers off above 50 km.

[96] Reviewing the precision determinations, the estimate from the retrieval leads to smaller values than are derived from comparisons with radiosondes, lidars, or ECMWF analyses. The former two have differences due to not being simultaneous and colocated, and perhaps from underestimates of their errors. The ECMWF analyses can be interpolated to the time and place of the HIRDLS measurements, but there are differences in vertical resolution that have not been treated, as well as effects of different view directions. HIRDLS comparisons with itself, where scans are spatially very close together but 99 min apart, leads to results close to the estimates in the lower stratosphere, and not too much above under quiet conditions. The sensitivity to small-scale variations, which in general will have short time constants, and the results of the self-comparison for different seasons, suggest that the observed increase with altitude is due to rapidly changing features not resolved in the GMAO data. The estimated values are probably the intrinsic repeatability for slowly varying features, but that may be somewhat academic.

10. Summary and Conclusions

10.1. Summary

[97] The V2.04.09 data described here represent a snapshot in time of the HIRDLS results. The blockage of the optical train was an unexpected and unprecedented event. The situation had to be diagnosed and separated into addressable problems. Concepts for corrections had to be put forth, algorithms written and tested, then implemented in the operational processing system, and the results evaluated. Multiple iterations have been required. The quantities that have been described here, especially temperature and ozone, are retrieved from channels with the largest radiances, and thus the greatest tolerance for errors. The fact that the biases for those quantities are not large and are very repeatable suggests that the sources of the systematic effects can be found and removed.

[98] This paper has presented the evaluation of the temperature data. They show HIRDLS temperatures within ±2 K of standards from the upper troposphere to the upper stratosphere, apart from the tropical tropopause region, with no indication of latitudinal variations of biases or temporal drifts. Other studies show that the data can reproduce the atmospheric horizontal and vertical structure. The noise levels are in line with predictions, and low enough to make the data highly useful. Perhaps most critical, they show an ability to resolve small vertical scales. In a related investigation, *Alexander et al.* [2008] have demonstrated that HIRDLS data capture atmospheric wave motions with vertical variations of only a few kilometers, shorter than previously available.

[99] In a companion paper *Massie et al.* [2007] have demonstrated HIRDLS' ability to observe subvisible cirrus clouds, polar stratospheric clouds (PSCs) and aerosols. They also show that there are sufficient cloud-free regions to allow retrievals into the upper troposphere a reasonable fraction of the time.

[100] *Nardi et al.* [2008] describes the ozone validation and presents its results. Over a deep layer of the atmosphere, from 50 to 2 hPa, ozone is within 5–10% of sonde or lidar standards, and values within 10–20% from 50 to 100 hPa. They also show the ability to capture small-scale features.

Relative measurements at pressures >100 hPa also appear useful.

[101] The characteristics of the nitric acid data have been detailed by *Kinnison et al.* [2008]. Retrievals correctly reproduce the latitudinal and seasonal variations of nitric acid, although there is a considerable low bias under all conditions. The bias appears to be uniform with latitude and time. The values are most precise and reliable between 100 and 10 hPa, with empirically estimated precision 10–30%.

[102] However, a radiometric error that can be tolerated for these quantities appears to be too large for the channels leading to water vapor, methane, nitrogen dioxide and the other species. What has been learned to date is being used to work toward reducing the errors in the radiance, so that useful values for other species can be recovered, and systematic errors in present quantities can be greatly reduced. New, improved versions are under development.

[103] Being limited to the single azimuth angle (−47° line of sight) means that the objectives of looking at smaller longitudinal scales will not be possible, nor will coverage over the Antarctic continent. While this is very disappointing, HIRDLS can still meet the majority of its most important science objectives.

[104] The high vertical resolution opens some unprecedented doors in looking for thin laminae in the upper troposphere/lower stratosphere that may be involved in stratosphere-troposphere exchange. The ability to look at this region was one of the main objectives of HIRDLS, and this has now been met by the species mentioned. It is hoped that soon other species will be added to this list of gases that may be used as tracers of air motions.

[105] The high vertical resolution will also allow much more detailed and global studies of shorter-scale gravity and Kelvin waves. The loss of azimuthal coverage can be partially compensated by more closely spaced profiles along the orbit track, which has some advantages when looking at gravity wave questions, and other dynamical features where the ratio of vertical to horizontal resolution is desired to be comparable to the ratio of Brunt-Vaisala frequency to Coriolis parameter.

[106] The high vertical resolution may also allow the use of HIRDLS ozone in conjunction with column ozone measurements to derive an estimate of tropospheric ozone, by better locating the boundary between the troposphere and stratosphere.

[107] The HIRDLS V2.04.09 capabilities are summarized very briefly in Table 3. Anyone interested in the data should consult the papers mentioned for much greater detail.

10.2. Conclusions

[108] The HIRDLS instrument was designed to address a number of important problems, especially those concerning the region around the tropopause, and the UT/LS in general. All indications were that the instrument would meet or exceed its requirements, the lower than prescribed noise levels being an example. The calibration was carried out very successfully, as were all prelaunch tests.

[109] It was thus a severe blow when a blockage developed in the optical train during launch. By dint of much ingenuity and hard work, a set of correction algorithms has been developed and implemented. These were outlined above, and their effectiveness has been demonstrated by the temperature results shown, as well as the ozone, nitric acid and aerosol results cited.

[110] The conclusion is that these data show reasonable results for this stage in the development of the corrections. Improvement of correction algorithms continues, although the operational implementation of new algorithms takes time. The low noise and consistency of the biases are excellent indications of the underlying quality of the instrumental data.

[111] HIRDLS data will add unique features to the Aura data sets. In particular, the high vertical resolution and ability to see clouds and aerosols, as well as additional species, will make it an important addition to the Aura data. With these improvements, HIRDLS will provide data to support the Aura objectives and atmospheric research.

[112] **Acknowledgments.** It is impossible to acknowledge all the people who contributed in large and small ways to the development of the HIRDLS instrument, data reduction and correction software, and the validation reported here. We would specifically like to express our deep appreciation to our coinvestigators Paul Bailey, Byron Boville (deceased), James Holton (deceased), and Conway Leovy, as well as to James Hannigan, Glenn Jackson, Nicholas Koepp-Baker (deceased), Thomas Lauren, Aaron Lee, Claire Wilda, and Robert Wells. As described in section 4, we have relied on data obtained when the Aura spacecraft is pitched down from its normal orientation. This pitch maneuver disrupts the observations of the other instruments on Aura. The HIRDLS team is very grateful that the other instrument teams have agreed to these pitch maneuvers for a few orbits 3 or 4 times a year. This work was supported in the U.S. by NASA under contract NAS5–97046, and in the U.K. by NERC under multiple contracts. The National Center for Atmospheric Research is sponsored by the National Science Foundation. We acknowledge the ECMWF for the use of their data, the Meteorological Office for the high-resolution sonde data, and the British Atmospheric Data Centre (BADC) for providing both of these data sets. The ACE mission is supported primarily by the Canadian Space Agency. Work at the Jet Propulsion Laboratory, California Institute of Technology, was carried out under a contract with NASA.

References

Alexander, M. J., et al. (2008), Global estimates of gravity wave momentum flux from High Resolution Dynamics Limb Sounder observations, *J. Geophys. Res.*, *113*, D15S18, doi:10.1029/2007JD008807.

Bailey, P., and J. C. Gille (1986), Inversion of the limb radiance measurements: An operational algorithm, *J. Geophys. Res.*, *91*(D2), 2757–2774, doi:10.1029/JD091iD02p02757.

Barnett, J. J., et al. (2003), Pre-launch calibration of the NASA AURA HIRDLS instrument, *Proc. SPIE Int. Soc. Opt. Eng.*, *5152*, 172–180, doi:10.1117/12.507496.

Bernath, P. F., et al. (2005), Atmospheric Chemistry Experiment (ACE): Mission overview, *Geophys. Res. Lett.*, *32*, L15S01, doi:10.1029/2005GL022386.

Borsche, M., G. Kirchengast, and U. Foelsche (2007), Tropical tropopause climatology as observed with radio occultation measurements from CHAMP compared to ECMWF and NCEP analyses, *Geophys. Res. Lett.*, *34*, L03702, doi:10.1029/2006GL027918.

Eden, T. D., Jr., et al. (2003a), Spectral characterization of the HIRDLS flight instrument from pre-launch calibration data, *Proc. SPIE Int. Soc. Opt. Eng.*, *5152*, 214–222, doi:10.1117/12.507673.

Eden, T. D., Jr., J. C. Gille, J. J. Barnett, P. Arter, C. L. Hepplewhite, C. W. P. Palmer, D. M. Peters, R. E. J. Watkins, and J. G. Whitney (2003b), Radiometric calibration of the HIRDLS flight instrument from pre-launch calibration data, *Proc. SPIE Int. Soc. Opt. Eng.*, *5152*, 231–237, doi:10.1117/12.507670.

Eden, T., J. C. Gille, J. J. Barnett, C. L. Hepplewhite, C. W. P. Palmer, and J. G. Whitney (2005a), HIRDLS proto-flight model spectral characterization from pre-launch calibration data, Proc, *SPIE Int. Soc. Opt. Eng.*, *5338*, K1–K13.

Eden, T., J. C. Gille, J. J. Barnett, C. L. Hepplewhite, C. W. P. Palmer, and J. G. Whitney (2005b), HIRDLS proto-flight model radiometric calibration from pre-launch calibration data, Proc, *SPIE Int. Soc. Opt. Eng.*, *5338*, L1–L11.

Edwards, D. P., J. C. Gille, P. L. Bailey, and J. J. Barnett (1995), Selection of sounding channels for the High Resolution Dynamics Limb Sounder, *Appl. Opt.*, *34*, 7006–7017.

Fleming, E., S. Chandra, J. Barnett, and M. Corney (1990), Zonal mean temperature, pressure, zonal wind and geopotential height as functions of latitude, *Adv. Space Res.*, *10*, 11–53, doi:10.1016/0273-1177(90)90386-E.

Francis, G. L., D. P. Edwards, A. Lambert, C. M. Halvorson, J. M. Lee-Taylor, and J. C. Gille (2006), Forward modeling and radiative transfer for the NASA EOS-Aura High Resolution Dynamics Limb Sounder (HIRDLS) instrument, *J. Geophys. Res.*, *111*, D13301, doi:10.1029/2005JD006270.

Gille, J. C., and J. J. Barnett (1992), The High Resolution Dynamics Limb Sounder (HIRDLS): An instrument for the study of global change, in *The Use of EOS for Studies of Atmospheric Physics*, edited by J. C. Gille and G. Visconti, pp. 433–450, North Holland, Amsterdam.

Gille, J. C., and F. B. House (1971), On the inversion of limb radiance measurements, I. Temperature and thickness, *J. Atmos. Sci.*, *28*, 1427–1442, doi:10.1175/1520-0469(1971)028<1427:OTIOLR>2.0.CO;2.

Gille, J. C., and J. M. Russell III (1984), The limb infrared monitor of the stratosphere: Experiment description, performance and results, *J. Geophys. Res.*, *89*, 5125–5140, doi:10.1029/JD089iD04p05125.

Gille, J. C., P. L. Bailey, R. A. Craig, F. B. House, and G. P. Anderson (1980), Sounding the stratosphere and mesosphere by infrared limb scanning from space, *Science*, *208*, 397–399, doi:10.1126/science.208.4442.397.

Gille, J. C., J. J. Barnett, J. C. Whitney, M. A. Dials, D. M. Woodard, W. Rudolf, A. Lambert, and W. Mankin (2003), The High Resolution Dynamics Limb Sounder (HIRDLS) experiment on Aura, *Proc. SPIE Int. Soc. Opt. Eng.*, *5152*, 162–171, doi:10.1117/12.507657.

Global Modeling and Assimilation Office (2007), Documentation of the impact of system upgrades to GEOS-5.1.0 from GEOS-5.0.1, NASA, Greenbelt, Md.

Hepplewhite, C. L., J. Barnett, R. W. J. Watkins, F. Row, R. Wolfenden, K. Djotni, and P. Arter (2003), NASA Aura HIRDLS instrument calibration facility, *Proc. SPIE Int. Soc. Opt. Eng.*, *5152*, 181–192, doi:10.1117/12.507277.

Kinnison, D. E., et al. (2008), Global observations of HNO_3 from the High Resolution Dynamics Limb Sounder (HIRDLS): First results, *J. Geophys. Res.*, doi:10.1029/2007JD008814, in press.

Lambert, A., P. L. Bailey, D. P. Edwards, J. C. Gille, B. R. Johnson, C. M. Halvorson, S. T. Massie, and K. A. Stone (1999), HIRDLS Level-2 Algorithm Theoretical Basis Document, NASA Goddard Space Flight Cent., Greenbelt, Md. (Available at http://eospso.gsfc.nasa.gov/eos_homepage/for_scientists/atbd/docs/HIRDLS/ATBD-HIR-02.pdf)

Leblanc, T., I. S. McDermid, A. Hauchecorne, and P. Keckhut (1998), Evaluation of optimization of lidar temperature analysis algorithms using simulated data, *J. Geophys. Res.*, *103*(D6), 6177–6187, doi:10.1029/97JD03494.

Lindzen, R., and M. Fox-Rabinovitz (1989), Consistent vertical and horizontal resolution, *Mon. Weather Rev.*, *117*, 2575–2583, doi:10.1175/1520-0493(1989)117<2575:CVAHR>2.0.CO;2.

Massie, S., et al. (2007), High Resolution Dynamics Limb Sounder observations of polar stratospheric clouds and subvisible cirrus, *J. Geophys. Res.*, *112*, D24S31, doi:10.1029/2007JD008788.

Moorhouse, J. L., et al. (2003), HIRDLS field of view calibration techniques and results, *Proc. SPIE Int. Soc. Opt. Eng.*, *5152*, 193–203, doi:10.1117/12.507315.

Nardi, B., et al. (2008), Initial validation of ozone measurements from the High Resolution Dynamic Limb Sounder (HIRDLS), *J. Geophys. Res.*, *113*, D16S36, doi:10.1029/2007JD008837.

Ridolfi, M., et al. (2007), Geophysical validation of temperature retrieved by the ESA processor from MIPAS/ENVISAT atmospheric limb-emission measurements, *Atmos. Chem. Phys.*, *7*, 4459–4487.

Rodgers, C. D. (2000), *Inverse Methods for Atmospheric Sounding, Theory and Practice*, World Sci., Hackensack, N. J.

Schwartz, M. J., et al. (2008), Validation of the Aura Microwave Limb Sounder temperature and geopotential height measurements, *J. Geophys. Res.*, *113*, D15S11, doi:10.1029/2007JD008783.

Sica, R. J., et al. (2007), Validation of the Atmospheric Chemistry Experiment (ACE) version 2.2 temperature using ground-based and space-borne measurements, *Atmos. Chem. Phys. Discuss.*, *7*, 12,463–12,539.

Simmons, A., M. Hortal, G. Kelly, A. McNally, A. Untch, and S. Uppala (2003), Analyses and forecasts of stratospheric winter polar vortex breakup: September 2002 in the Southern Hemisphere and related events from ECMWF operations and ERA-40, *ERA-40 Proj. Rep. Ser., 5,* Eur. Cent. for Med.-Range Weather Forecasts, Reading, U.K.

Simmons, A., M. Hortal, G. Kelly, A. McNally, A. Untch, and S. Uppala (2005), ECMWF analyses and forecasts of stratospheric winter polar vortex breakup: September 2002 in the Southern Hemisphere and related events, *J. Atmos. Sci.*, *62*(3), 668–689.

Susskind, J., C. Barnett, and J. Blaisdell (2003), Retrieval of Atmospheric and Surface Parameters From AIRS/AMSDU/HSB Data in the Presence of Clouds, *IEEE Trans. Geosci. Remote Sens.*, *41*(2), 390–409, doi:10.1109/TGRS.2002.808236.

Taylor, F. W., et al. (1993), Remote sensing of atmospheric structure and composition by pressure modulator radiometry from space: The ISAMS experiment on UARS, *J. Geophys. Res.*, *98*(D6), 10,799–10,814, doi:10.1029/92JD03029.

M. Barker, J. Chow, W. Rudolf, and J. Serafin, Lockheed Martin Advanced Technology Center, Palo Alto, CA 94304, USA.

J. Barnett, C. Hepplewhite, J. Moorhouse, R. Watkins, and J. Whitney, Department of Physics, Oxford University, Oxford OX1 3PU, UK.

P. Bernath, Department of Chemistry, University of York, York YO10 5DD, UK.

C. Boone, Department of Chemistry, University of Waterloo, Waterloo, ON N2L 3G1, Canada.

C. Cavanaugh, M. Coffey, C. Craig, T. Eden, D. P. Edwards, G. Francis, C. Halvorson, R. Khosravi, D. Kinnison, A. Lambert, W. Mankin, S. Massie, B. Nardi, and D. Packman, National Center for Atmospheric Research, Boulder, CO 80307, USA.

J. Craft, V. Dean, J. Gille, C. Krinsky, J. Loh, J. McInerney, B. Torpy, and G. Young, Center for Limb Atmospheric Sounding, University of Colorado, Boulder, CO 80309, USA. (gille@ucar.edu)

M. Dials, Ball Aerospace and Technologies Corporation, Boulder, CO 80301, USA.

L. Harvey and C. Randall, Laboratory for Atmospheric and Space Physics, University of Colorado, Boulder, CO 80303, USA.

L. Lyjak, National Weather Service, NOAA, Silver Spring, MD 20910, USA.

J. Reburn and A. Waterfall, Rutherford Appleton Laboratory, Didcot OX11 0QX, UK.

M. Schwartz, Jet Propulsion Laboratory, California Institute of Technology, Pasadena, CA 91109, USA.

K. Stone, ERT, Inc., 16800 East Centretech Parkway, Aurora, CO 80011, USA.

K. Walker, Department of Physics, University of Toronto, Toronto, ON M5S 1A7, Canada.